

# Linear response pCCD-based methods: LR-pCCD and LR-pCCD+S approaches for the efficient and reliable modelling of excited state properties

Somayeh Ahmadkhani,<sup>1</sup> Katharina Boguslawski,<sup>1</sup> and Paweł Tecmer<sup>1</sup>

*Institute of Physics, Faculty of Physics, Astronomy and Informatics, Nicolaus Copernicus University in Toruń, Grudziądzka 5, 87-100 Toruń, Poland*

(Dated: 15 November 2024)

**Abstract:** In this work, we derive working equations for the Linear Response pair Coupled Cluster Doubles (LR-pCCD) ansatz and its extension to singles (S), LR-pCCD+S. These methods allow us to compute electronic excitation energies and transition dipole moments based on a pCCD reference function. We benchmark the LR-pCCD+S model against the linear response coupled-cluster singles and doubles method for modeling electronic spectra (excitation energies and transition dipole moments) of the BH, H<sub>2</sub>O, H<sub>2</sub>CO, and furan molecules. We also analyze the effect of orbital optimization within pCCD on the resulting LR-pCCD+S transition dipole moments and oscillator strengths and perform a statistical error analysis. We show that the LR-pCCD+S method can correctly reproduce the transition dipole moments features, thus representing a reliable and cost-effective alternative to standard, more expensive electronic structure methods for modeling electronic spectra of simple molecules. Specifically, the proposed models require only mean-field-like computational cost, while excited-state properties may approach the CCSD level of accuracy. Moreover, we demonstrate the capability of our model to simulate electronic transitions with non-negligible contributions of double excitations and the electronic spectra of polyenes of various chain lengths, for which standard electronic structure methods perform purely.

## I. INTRODUCTION

Electronic spectroscopy plays a pivotal role in various scientific disciplines, from chemistry to physics, biology, and astronomy. Electronic spectra provide a fingerprint of an investigated system. They are crucial for understanding the behavior of electrons in atoms and molecules and the design of new complexes and materials. Experimentally, the electronic spectrum is recorded via absorption or emission processes. The emission spectrum is generated when electrons transition from higher to lower energy levels, emitting photons. The absorption spectrum is produced by electrons absorbing photons to move from lower to higher energy levels. An absorption spectrum is essentially the reverse of an emission spectrum, both provide characteristic molecular features.<sup>1,2</sup>

In recent years, quantum chemistry has become increasingly essential in predicting and interpreting atomic and molecular electronic spectra.<sup>3,4</sup> Two main families of quantum chemistry methods emerged: density functional theory approximations (DFAs) and wave function theory (WFT) based methods. While DFAs are generally more cost-effective, it is well-accepted that WFT provides more reliable results. Specifically, the quality of DFAs' electronic spectra strongly depends on the applied approximation to the exchange–correlation functional. Several classes of approximate exchange–correlation functionals have been developed so far, ranging from the simplest local and semi-local, to hybrid, meta-hybrid, and double-hybrid, to more complex range-separated exchange–correlation functionals.<sup>5</sup> While some

of the approximations to the exchange–correlation functional provide reliable results for molecular structures, others perform well in predicting electronic excitation energies.<sup>6,7</sup> However, none of them is universal. Particularly challenging for DFAs are so-called multi-reference systems with a significant amount of strong electron correlation. Such strongly-correlated electrons can be encountered, for instance, when stretching multiple bonds or in extended  $\pi$ -systems.

In WFT, the exact solution to the electronic Schrödinger equation (in a given basis) can be obtained from the full configuration interaction (FCI) approach. Unfortunately, such calculations are computationally feasible only for some small model systems, comprising usually less than 20 electrons and/or orbitals, as the number of degrees of freedom scales binomially with system size. That technical deficiency led to the development of approximate WFT-based methods (including the hybrid WFT/DFA methods<sup>8</sup>), among which the coupled cluster (CC) theory<sup>9</sup> emerged as the most promising one. Conventional CC theory, like the coupled cluster singles and doubles (CCSD) and CCSD with perturbative triples (CCSD(T)<sup>10</sup>), can be used to accurately model large molecular systems whose electronic structures are well-represented by a single Slater determinant, that is, dominated by dynamic electron correlation effects. The pair Coupled-Cluster Doubles<sup>11,12</sup> (pCCD) model represents a cost-effective alternative for reliable description of strongly correlated systems.<sup>13</sup> Combined with an efficient orbital optimization protocol,<sup>14–17</sup> and dynamic energy correction<sup>18–23</sup> pCCD-based approaches represent a versatile tool for large-scale modeling of complex sys-

tems.<sup>24–27</sup>

Employing the equation of motion (EOM) formalism<sup>28–30</sup> on top of a pCCD reference function allows us to obtain a large number of electronically excited states in one single calculation.<sup>31–33</sup> The resulting excitation energies are size-intensive. An advantage of EOM-pCCD-based methods over the standard EOM-CC approaches is the low computational cost and the ability to model electronically excited states of large  $\pi$ -conjugated systems<sup>34</sup>, where the electron pair excitation energies can play a significant role.<sup>31,33</sup> Unfortunately, the computation of oscillator strengths from EOM-CC methods, including the pCCD-based variants, requires the determination of both the right (as for excitation energies) and left eigenvectors of the EOM-CC equations, which essentially doubles the cost of excited-state calculations compared to the calculations of excitation energies only.<sup>29</sup> Alternatively, the electronic spectra can be obtained from the linear response (LR) formulation of CC theory (LR-CC).<sup>35–38</sup> In that case, the excitation energies remain identical with EOM-CC,<sup>38,39</sup> the computation of transition dipole moments still requires left and right eigenvectors, but the resulting transition dipole moments are size-intensive.<sup>38,40</sup> The standard CCSD-based excitation energies can be further corrected for triple excitations using iterative<sup>41</sup> and non-iterative techniques<sup>42,43</sup>.

The exceptional performance of EOM-pCCD-based methods for modeling electronic excitation energies of complex systems<sup>31,33,44</sup> and the advantages of the LR-CC formalism motivate us to develop the LR-CC models based on a pCCD reference function (with and without orbital optimization). In this work, we provide working equations for the LR-pCCD and LR-pCCD+S (LR-pCCD with the inclusion of singly excited states) models. Our focus is on excited state properties, not excitation energies, which have been assessed before.<sup>31,33,44</sup> We benchmark the LR-pCCD+S transition dipole moments (TDM) and oscillator strengths (OS) against the LR-CCSD and EOM-CCSD results for small model systems and various basis set sizes. Finally, we show the ability of LR-pCCD+S to model electronic spectra of all trans-polyenes of different chain lengths.

## II. THEORY

### A. The pCCD ansatz

One of the most interesting recent developments in CC theory<sup>9,45,46</sup> is the pCCD ansatz<sup>11–13</sup>, which restricts the coupled cluster wave function ansatz to only electron pair excitations and overall zero-spin,

$$|\text{pCCD}\rangle = e^{\hat{T}_{\text{pCCD}}} |\text{HF}\rangle, \quad (1)$$

where  $|\text{HF}\rangle$  is some reference determinant (usually the Hartree–Fock determinant) and

$$\hat{T}_{\text{pCCD}} = \sum_{ai} t_{ii}^{a\bar{a}} \hat{P}_a^\dagger \hat{P}_i. \quad (2)$$

In the above equation,  $i, j, \dots (a, b, \dots)$  refer to the occupied (virtual) orbitals.  $\hat{P}_q^\dagger = \hat{q}_\uparrow^\dagger \hat{q}_\downarrow^\dagger$  and  $\hat{P}_p = \hat{p}_\uparrow \hat{p}_\downarrow$  are general pair creation ( $\hat{P}_q^\dagger$ ) and annihilation operators ( $\hat{P}_p$ ), respectively. pCCD represents a computationally attractive size-extensive model with mean-field-like scaling.<sup>11</sup> The variational orbital optimization<sup>12,14–17</sup> of the corresponding pCCD orbitals is often carried out to recover size-consistency.<sup>47,48</sup>

The pCCD state aligns with the weak formulation of the time-independent Schrödinger equation,

$$e^{-\hat{T}_{\text{pCCD}}} \hat{H}_0 |\text{pCCD}\rangle = E_0 e^{-\hat{T}_{\text{pCCD}}} |\text{pCCD}\rangle, \quad (3)$$

that is obtained by projecting the  $\langle \text{HF} |$  state from the left-hand-side as  $E_0 = \langle \text{HF} | \hat{H}_0 |\text{pCCD}\rangle$  and  $\hat{H}_0$  being the molecular Hamiltonian in its normal-product form,

$$\hat{H}_0 = \sum_{pq} f_p^q \{\hat{p}^\dagger \hat{q}\} + \frac{1}{2} \sum_{pqrs} V_{pqrs} \{\hat{p}^\dagger \hat{q}^\dagger \hat{s} \hat{r}\}, \quad (4)$$

where  $f_p^q$  and  $V_{pqrs}$  denote the Fock operator and two-electron integrals, respectively. The pCCD amplitudes,  $t_{ii}^{a\bar{a}}$ , are then obtained by projection,

$$\langle \mu | e^{-\hat{T}_{\text{pCCD}}} \hat{H}_0 |\text{pCCD}\rangle = 0, \quad (5)$$

where  $\langle \mu | = \langle \text{HF} | \hat{\tau}_\mu^\dagger$ , and  $\hat{\tau}_\mu^\dagger$  refers to the de-excitation operator, here,  $\hat{P}_i^\dagger \hat{P}_a$ .

### B. LR-pCCD and LR-pCCD+S

The basic response equation for arbitrary operators  $\hat{A}$  and  $\hat{B}$  is given by<sup>36,49</sup>

$$\langle \langle \hat{A}; \hat{B} \rangle \rangle = \sum_k \left\{ \frac{\langle 0 | \hat{A} | k \rangle \langle k | \hat{B} | 0 \rangle}{\omega - \omega_k + i\alpha} - \frac{\langle 0 | \hat{B} | k \rangle \langle k | \hat{A} | 0 \rangle}{\omega + \omega_k + i\alpha} \right\}, \quad (6)$$

where  $\langle 0 |$  and  $|k\rangle$  are the ground and excited states, respectively, and  $\alpha$  is a real positive infinitesimal to prevent divergence. Defining  $\langle \Lambda |$  as a dual-type vector to the pCCD wave function,

$$\langle \Lambda | = \langle \text{HF} | + \sum_{\mu} \bar{t}_{\mu} \langle \bar{\mu}_2 |, \quad (7)$$

satisfies the time-independent Schrödinger equation and the normalization condition<sup>36</sup>,

$$\langle \Lambda | \hat{H}_0 |\text{pCCD}\rangle = E_0, \quad (8)$$

$$\langle \Lambda | \text{pCCD}\rangle = 1, \quad (9)$$

where the index 2 in  $\langle\mu_2| = \langle\text{HF}|\tau_{\mu_2}^\dagger$  refers to pair de-excitations and  $\hat{t}_\mu$  are the Lagrange multipliers. Considering  $J_{\mu\nu}$  as a Jacobian matrix we will have,

$$\sum_\mu \hat{t}_\mu J_{\mu\nu} = \langle\text{HF}|\hat{H}_0, \hat{\tau}_\nu| \text{pCCD}\rangle. \quad (10)$$

In the presence of an external potential ( $\lambda\hat{V}$ ), applied to a molecular structure with  $\lambda$  intensity, Eqs. (5), (7), and (10) lead to

$$\frac{d}{d\lambda} \langle\Lambda(\lambda)|(\hat{H}_0 + \lambda\hat{V})| \text{pCCD}(\lambda)\rangle|_{\lambda=0} \approx \langle\Lambda|\hat{V}| \text{pCCD}\rangle. \quad (11)$$

Using the extended Hellmann–Feynman theorem, we can incorporate  $| \text{pCCD}\rangle$  and  $\langle\Lambda|$  states into the transition expectation value. According to Eq. (8), when the cluster operator is not truncated,  $| \text{pCCD}\rangle$  and  $\langle\Lambda|$  states represent exact normalized states. However, with a truncated cluster operator,  $\langle\Lambda|$  does not act as the adjoint of  $| \text{pCCD}\rangle$ . In this scenario, under the assumption of a time-independent perturbation limit, the response function corresponds to the results of Refs. 50,51 utilizing the Lagrangian technique approach<sup>36</sup>. In our case, the derivatives of molecular orbital coefficients with respect to the perturbation are ignored, and  $\Lambda$  contains the pair excitations only for all models.

The response function for an externally applied time-dependent potential  $\hat{B} \rightarrow \hat{V}_t$  is briefly derived in Ref. 49 for linear and quadratic terms. Since we are approximating the calculation to the linear part of the response function and using the coupled cluster reference wave function, the derivation of the equations is as follows

$$\begin{aligned} \langle\langle\hat{A}; \hat{V}^\omega\rangle\rangle &= \sum_n Y_n(\omega + i\alpha) \langle\bar{n}|\hat{A}| \text{pCCD}\rangle + \\ &\sum_n X_n(\omega + i\alpha) \langle\Lambda|[\hat{A}, \hat{\tau}_n]| \text{pCCD}\rangle, \end{aligned} \quad (12)$$

where  $\hat{V}^\omega$  is the Fourier transformation of the time-dependent potential  $\hat{V}_t = \int \exp(-i(\omega + i\alpha)t)\hat{V}^\omega d\omega$ . Assuming the diagonalization of the non-symmetric Jacobian matrix,

$$J_{nm} = (U^{-1}\hat{A}U)_{nm} = \delta_{nm}\omega_n, \quad (13)$$

the de-excited and excited states can be defined as  $\langle\bar{n}| = \sum_\nu U_{n\nu}^{-1}\langle\bar{\nu}|$  and  $\hat{\tau}_m = \sum_\mu \hat{\tau}_\mu U_{\mu m}$ , respectively. The  $X$  and  $Y$  vectors in Eq. (12) are then expressed in terms of the Jacobian matrix and excitation energies ( $\omega$ ),

$$X_\mu(\omega) = \sum_\nu (\mathbf{J} + (\omega + i\alpha)\mathbf{I})_{\mu\nu}^{-1} \xi_\nu, \quad (14)$$

and

$$\begin{aligned} Y_\mu(\omega) &= \sum_\nu \left( \langle\Lambda|[\hat{V}^\omega, \hat{\tau}_\nu]| \text{pCCD}\rangle + \sum_\gamma F_{\nu\gamma} X_\nu(\omega + i\alpha) \right) \times \\ &(\mathbf{J} + (\omega + i\alpha)\mathbf{I})_{\mu\nu}^{-1}. \end{aligned} \quad (15)$$

Explicit forms of LR-pCCD and LR-pCCD+S vectors and matrices are collected in Table I. More details related to the derivation of these vectors and matrices can be found in the SI.

### C. Excitation energies

Opposite to the EOM-CC approach, we don't need to diagonalize the effective Hamiltonian to obtain excitation energies using the LR-CC formalism. We should emphasize that the excitation energies and excited states are extracted from the diagonalized Jacobian matrix. It links the eigenvalues of the Jacobian with the underlying excited-state energies and associated eigenvectors with the excited-state wavefunctions. To clarify this further, we can rewrite the LR function from Eq. (6) as

$$\langle\langle\hat{A}; \hat{B}\rangle\rangle = \mathbf{A}^{[1]T} (\mathbf{E}^{[2]} - \omega \mathbf{S}^{[2]}) \mathbf{B}^{[1]}, \quad (16)$$

where  $\mathbf{A}^{[1]T}$  is the transposed one-dimensional array of  $\hat{A}$  components ( $\langle 0|\hat{A}|n\rangle, \langle n|\hat{A}|0\rangle$ ),  $\mathbf{B}^{[1]} = (\langle n|\hat{B}|0\rangle, \langle 0|\hat{B}|n\rangle)$ , and the term in parenthesis provides the excitation energies of the system. By considering this concept, we can rewrite the LR-CC function as follows

$$\langle\langle\hat{A}; \hat{V}^\omega\rangle\rangle = \eta^{\hat{A}} (\mathbf{E}^{[2]} - \omega \mathbf{S}^{[2]}) g^{\hat{V}^\omega}, \quad (17)$$

where  $\eta_i^{\hat{A}} = (\langle 0|[\hat{A}, \hat{\tau}_i]|0\rangle, \langle 0|[\hat{A}, \hat{\tau}_i^\dagger]|0\rangle)$  and  $g_i^{\hat{V}^\omega} = (\langle 0|[\hat{V}^\omega, \hat{\tau}_i]|0\rangle, \langle 0|[\hat{V}^\omega, \hat{\tau}_i^\dagger]|0\rangle)$ . As a result, we obtain the excitation energies of the system by diagonalizing  $(\mathbf{E}^{[2]} - \omega \mathbf{S}^{[2]})$ , where

$$\mathbf{E}^{[2]} = E_{\mu,\nu} = \begin{pmatrix} \langle 0|[[\hat{\tau}_\mu, \bar{H}_0], \hat{\tau}_\nu^\dagger]|0\rangle & \langle 0|[[\hat{\tau}_\mu, \bar{H}_0], \hat{\tau}_\nu]|0\rangle \\ \langle 0|[[\hat{\tau}_\mu^\dagger, \bar{H}_0], \hat{\tau}_\nu]|0\rangle & \langle 0|[[\hat{\tau}_\mu^\dagger, \bar{H}_0], \hat{\tau}_\nu^\dagger]|0\rangle \end{pmatrix}, \quad (18)$$

and

$$\mathbf{S}^{[2]} = S_{\mu,\nu} = \begin{pmatrix} \langle 0|[\hat{\tau}_\mu, \hat{\tau}_\nu^\dagger]|0\rangle & \langle 0|[\hat{\tau}_\mu, \hat{\tau}_\nu]|0\rangle \\ -\langle 0|[\hat{\tau}_\mu^\dagger, \hat{\tau}_\nu^\dagger]|0\rangle & -\langle 0|[\hat{\tau}_\mu^\dagger, \hat{\tau}_\nu]|0\rangle \end{pmatrix}. \quad (19)$$

The diagonal terms of the  $\mathbf{S}$  matrix contain single excitations and de-excitations. The off-diagonal terms of  $\mathbf{S}$  accommodate only pair excitations and de-excitations and are usually small.

Let's now consider the molecular Hamiltonian in its normal-product form  $\hat{H}_0$  instead of the  $\hat{A}$  operator and represent the  $\hat{B}$  operator by any external potential operator. Now, Eq. (17) can be simplified such that  $\mathbf{E}$  will refer to the Jacobian matrix, and  $\mathbf{S}$  would become the identity matrix (see also Eq. (4.36) of Ref. 38). Specifically for the pair and single excitation operators and effective Hamiltonian, the following relations take place,

$$\begin{aligned} \hat{\tau}_{\nu_2} &= \hat{P}_b^\dagger \hat{P}_j, & \hat{\tau}_{\nu_1} &= \hat{b}^\dagger \hat{j}, \\ \bar{H}_0 &= e^{-\hat{T}_{\text{pCCD}}} \hat{H}_0 e^{\hat{T}_{\text{pCCD}}} \\ &= \hat{H}_0 + [\hat{H}_0, \hat{T}_{\text{pCCD}}] + \dots \end{aligned} \quad (20)$$

TABLE I. Response vectors and matrices for the LR-pCCD and LR-pCCD+S equations. Indices  $n=1$  and  $n=2$  refer to single and pair excitations (de-excitation) with respect to the  $\tau_{\mu n}$  ( $\tau_{\nu n}^\dagger$ ) operator. For more details see Ref. 36.

Name	LR-pCCD	LR-pCCD+S
$\bar{A}$	$= e^{-\hat{T}_{\text{pCCD}}} \hat{A} e^{\hat{T}_{\text{pCCD}}}$	$e^{-\hat{T}_{\text{pCCD}}} \hat{A} e^{\hat{T}_{\text{pCCD}}}$
$\eta_\nu^{\hat{A}}$	$= \langle \text{HF}   [\hat{A}, \hat{\tau}_{\nu 2}]   \text{pCCD} \rangle$	$\langle \text{HF}   [\hat{A}, \hat{\tau}_{\nu 2}]   \text{pCCD} \rangle, \quad \langle \text{HF}   [\hat{A}, \hat{\tau}_{\nu 1}]   \text{pCCD} \rangle$
$\xi_\mu^{\hat{A}}$	$= \langle \bar{\mu}_2   \bar{A}   \text{pCCD} \rangle$	$\langle \bar{\mu}_1   \bar{A}   \text{pCCD} \rangle, \quad \langle \bar{\mu}_2   \bar{A}   \text{pCCD} \rangle$
$F_{\mu\nu}$	$= \langle \Lambda   [[\hat{H}_0, \hat{\tau}_{\nu 2}], \hat{\tau}_{\mu 2}]   \text{pCCD} \rangle$	$\langle \Lambda   [[\hat{H}_0, \hat{\tau}_{\nu 1}], \hat{\tau}_{\mu 1}]   \text{pCCD} \rangle, \quad \langle \Lambda   [[\hat{H}_0, \hat{\tau}_{\nu 1}], \hat{\tau}_{\mu 2}]   \text{pCCD} \rangle$ $\langle \Lambda   [[\hat{H}_0, \hat{\tau}_{\nu 2}], \hat{\tau}_{\mu 1}]   \text{pCCD} \rangle, \quad \langle \Lambda   [[\hat{H}_0, \hat{\tau}_{\nu 2}], \hat{\tau}_{\mu 2}]   \text{pCCD} \rangle$
$J_{\mu\nu}$	$= \langle \text{HF}   [[\hat{H}_0, \hat{\tau}_{\nu 2}], \hat{\tau}_{\mu 2}]   \text{pCCD} \rangle$	$\langle \text{HF}   [[\hat{H}_0, \hat{\tau}_{\nu 1}], \hat{\tau}_{\mu 1}]   \text{pCCD} \rangle, \quad \langle \text{HF}   [[\hat{H}_0, \hat{\tau}_{\nu 1}], \hat{\tau}_{\mu 2}]   \text{pCCD} \rangle$ $\langle \text{HF}   [[\hat{H}_0, \hat{\tau}_{\nu 2}], \hat{\tau}_{\mu 1}]   \text{pCCD} \rangle, \quad \langle \text{HF}   [[\hat{H}_0, \hat{\tau}_{\nu 2}], \hat{\tau}_{\mu 2}]   \text{pCCD} \rangle$

Thus, we can investigate the excitation energies using all standard CC flavors, including pCCD models, by diagonalizing the Jacobian matrix,

$$(\hat{J} - \omega \mathbf{I}) \mathbf{X} = 0. \quad (21)$$

The explicit Jacobian matrix elements derived for the pCCD and pCCD+S models are provided in the last row of Table I. To diagonalize such a Jacobian matrix, we can use the non-symmetric Davidson method<sup>21,52</sup>. We should stress here that EOM-pCCD and LR-pCCD trivially have the same set of eigenvalues (excitation energies) as the diagonalization problems are equivalent. However, EOM-pCCD+S and LR-pCCD+S slightly differ in their excitation spectra as we only consider the Jacobian in the latter, while the former contains a non-zero first column in the effective Hamiltonian to be diagonalized.<sup>31,32</sup> These differences in excitation energies are minor (a few  $\mu E_h$ ) and orders of magnitude smaller than the accuracy of excitation energies.

#### D. Transition matrix elements

To study the excited state's properties, we need to align the excitation properties with those of the ground state. For that purpose, we use transition matrices that transfer specific ground state operator effects to the excited states. We need the excitation energies and vectors derived in section II C to achieve that.

The linear response function of Eq. (6) exhibits poles at energies  $\pm \omega_k$ . By evaluating the residues of these poles, we can straightforwardly obtain transition matrix elements. That involves approximating the frequencies of the linear response function in Eq. (12) by the pole

values, leading to the following relation,

$$\begin{aligned} \langle 0 | \hat{A} | k \rangle \langle k | \hat{B} | 0 \rangle &= \lim_{\omega \rightarrow \omega_k} (\omega - \omega_k) \langle \langle \hat{A}; \hat{B} \rangle \rangle = \\ &= - \sum_n \left\{ \langle \bar{n} | \hat{A} | \text{pCCD} \rangle (\omega - \omega_n)^{-1} F_{\nu n} + \right. \\ &\quad \left. \langle \Lambda | [\hat{A}, \hat{\tau}_n] | \text{pCCD} \rangle - X_\nu^{\hat{A}}(-\omega_n) F_{\nu n} \right\} \langle n | \hat{B} | 0 \rangle, \quad (22) \end{aligned}$$

where  $n$  is the total number of roots,  $k$  denotes the eigenvector, and  $\nu$  is the index of Jacobian matrix element. The above transition matrix could be written as

$$\begin{aligned} \langle 0 | \hat{A} | k \rangle \langle k | \hat{B} | 0 \rangle &= \left\{ \langle \Lambda | [\hat{A}, \hat{\tau}_k] | \text{pCCD} \rangle - \right. \\ &\quad \left. \sum_\nu (-\hat{J} + \omega \mathbf{I})_{\mu\nu}^{-1} \langle \bar{\nu} | \hat{A} | \text{pCCD} \rangle \langle \Lambda | [[\hat{H}_0, \hat{\tau}_\nu], \hat{\tau}_k] | \text{pCCD} \rangle \right\} \langle k | \hat{B} | 0 \rangle, \quad (23) \end{aligned}$$

where  $\hat{A}$  and  $\hat{B}$  are arbitrary operators,  $\hat{H}_0$  the Hamiltonian of Eq. (4),  $\hat{J}$  is the coupled cluster Jacobian, and  $|\text{pCCD}\rangle$  denotes the pCCD wave function (in the canonical or pCCD orbital basis). The operators  $\hat{A}$  and  $\hat{B}$  can define various properties such as transition dipole moment (TDM), polarizability<sup>53,54</sup>, and excited density matrix (EDM), among others.

#### E. Transition dipole moment and related properties

The TDM, in the absence of any external potential, can be obtained using only the  $\hat{A}$ -dependent part of Eq. (23) according to the following equation

$$\begin{aligned} \Gamma_{0 \rightarrow k}^{\hat{A}} &= \langle 0 | \hat{A} | k \rangle \\ &= \langle \Lambda | [\hat{A}, \hat{\tau}_k] | \text{pCCD} \rangle - \\ &= \sum_\nu (-\hat{J} + \omega \mathbf{I})_{\mu\nu}^{-1} \langle \bar{\nu} | \hat{A} | \text{pCCD} \rangle \langle \Lambda | [[\hat{H}_0, \hat{\tau}_\nu], \hat{\tau}_k] | \text{pCCD} \rangle. \quad (24) \end{aligned}$$

Using dipole operators, we can obtain the TDM of selected excited states. An intrinsic feature of choosing pCCD as the reference wave function—in contrast to CCSD-based approaches—is that the Jacobian becomes approximately symmetric, and we can approximate transition dipole moment using only the right eigenvectors without significantly deteriorating the accuracy. This approximation allows us to keep the computational cost to  $\mathcal{O}(o^2v^2)$  (see below). Similarly, the oscillator strength (OS) and dipole strength (DS) can be determined using Eq. (24) and the following relations,

$$\text{OS} = \frac{2}{3}\omega_k\Gamma_{0\rightarrow k}^\mu\Gamma_{0\rightarrow k}^\mu, \quad (25)$$

$$\text{DS} = \Gamma_{0\rightarrow k}^\mu\Gamma_{0\rightarrow k}^\mu, \quad (26)$$

where  $\omega_k$  are the eigenvalues of the Jacobian (excitation energies), and  $\Gamma_{0\rightarrow k}^\mu$  refers to the TDM elements.

### F. Computational scaling

Our pCCD-based linear response models feature a formal computational scaling of  $\mathcal{O}(o^2v^2)$  (with some prefactor), neglecting the 4-index transformation of the electron repulsion integrals (ERI), which can be further reduced by working with Cholesky-decomposed ERI. Thus, our LR-pCCD-based models are computationally more efficient than the standard LR-CCSD or EOM-CCSD models, which are of the order of  $\mathcal{O}(o^2v^4)$ . Furthermore, we can store the whole Jacobian (in principle, we can also exactly diagonalize it and have access to all eigenvalues and—left and right—eigenvectors) as it scales as  $\mathcal{O}(2 * o^2v^2)$  in terms of memory.

## III. COMPUTATIONAL DETAILS

All pCCD-based calculations were performed in the developer version of the PYBEST v2.1.0.dev0 software package.<sup>24,55</sup> The structural parameters for the small molecules ( $\text{H}_2\text{O}$ , BH,  $\text{H}_2\text{CO}$ , and furan) were taken from Refs. 56,57. We computed vertical excitation energies for these systems and explored different basis set variants ranging from cc-pVDZ to cc-pVQZ<sup>58</sup> and aug-cc-pVTZ.<sup>59</sup> To compare vertical excitation energies with a double electron transfer character to the CC2 and CC3 literature data, we employed the def2-TZVP basis sets.<sup>60</sup> The 1  $A_g^-$  ( $S_0$ ) ground state structures of all-trans polyenes were taken from Ref. 61. For these systems, we used a cc-pVDZ basis set.

In all our LR-pCCD+S calculations, we used the frozen core approximation (1s orbitals of C, O, and N were kept frozen) and tested two orbital sets: the canonical HF orbitals and the natural pCCD-optimized orbitals. For the latter, we employed a variation orbital optimization protocol<sup>14,17</sup> as implemented in PYBEST.

The reference EOM-CCSD calculations were carried out in the MOLPRO2020 software package<sup>62–64</sup> and the reference LR-CCSD and CCSDR(3) calculations<sup>42</sup> in the DALTON2020 software package<sup>65,66</sup> utilizing the same basis sets and structures as in PYBEST.

## IV. RESULTS AND DISCUSSION

In this section, we assess the quality of LR-pCCD+S TDMs (Eq. (24)), OSs (Eq. (25)), and DSs (SI) (Eq. (26)) by comparing them to other well-established quantum chemistry methods (EOM-CCSD and LR-CCSD) and when possible to experiment. Our analysis is divided into three parts: (a) molecules with a dominant single electron transfer, (b) molecules with a significant admixture of double electron excitations, and (c) polymer chains.

### A. Single electron excitation energies

We start our excited state property analysis by modeling electronic spectra using LR-CCSD and EOM-CCSD as reliable references, for which, triple excitations have negligible effects (see Tables S1-S4 of the SI). Specifically, we focus on the TDMs and OSs of the low-lying excited states of BH, water ( $\text{H}_2\text{O}$ ), formaldehyde ( $\text{H}_2\text{CO}$ ), and furan ( $\text{C}_4\text{H}_4\text{O}$ ) using different basis sets. We investigate two sets of LR-pCCD+S calculations, one where we utilize the HF canonical orbitals and the other where we employ the natural pCCD orbitals (denoted as LR-pCCD+S(HF) and LR-pCCD+S(pCCD), respectively). The performance of LR-pCCD results for these systems is illustrated in Figures 1–4. The corresponding numerical data, including excitation energies, TDMs, OSs, and DSs, are provided in Tables S1–S4 of the SI.

For the BH molecule, shown in Figure 1, the first ( $3\sigma \rightarrow 1\pi$ ) and third ( $3\sigma \rightarrow 2\pi$ ) electronic transitions exhibit almost the same excited state properties, while the second transition ( $3\sigma \rightarrow 4\sigma$ ) shows the largest values for TDM and OS. However, when the basis set is changed from cc-pVDZ to cc-pVTZ to cc-pVQZ, the difference in second excited state decreases, and LR-pCCD+S approaches LR-CCSD and EOM-CCSD.

Similarly, a good agreement is obtained for the formaldehyde molecule, where the canonical HF LR-pCCD+S excited state properties agree very well with the reference LR-CCSD and EOM-CCSD values and trends for all investigated basis sets (cf. Figure 2). Figure 2 highlights the small deviations occurring between methods even for larger basis set sizes.

We observe a somehow stronger excited-states property dependence on the basis set for the water and furan molecules shown in Figures 3 and 4, respectively. Specifically, the TDMs and OSs quantitatively change when moving from the cc-pVDZ to the cc-pVTZ basis set. Nonetheless, LR-pCCD+S predicts a qualitatively correct picture of TDMs and derived properties (OS) for

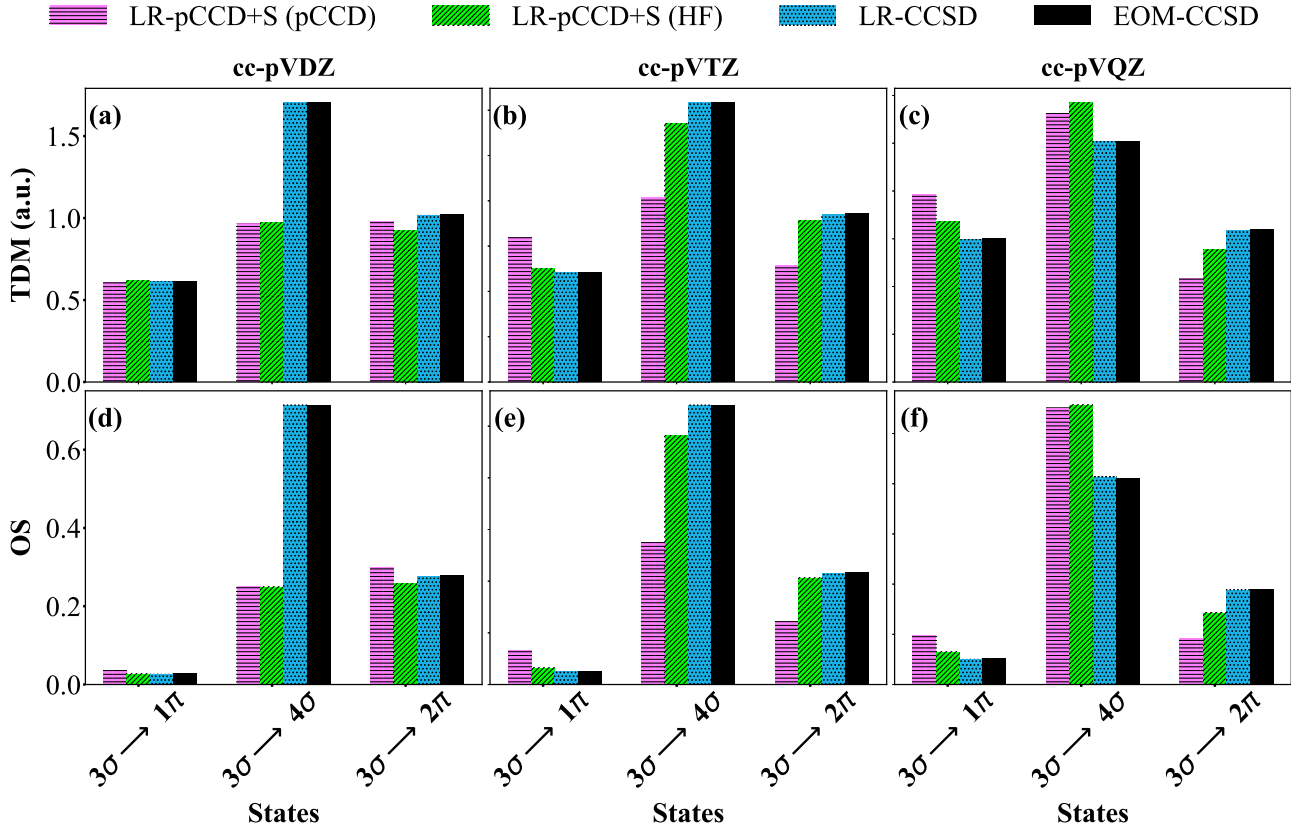


FIG. 1. LR-pCCD+S(HF), LR-pCCD+S(pCCD), LR-CCSD, and EOM-CCSD TDM and OS for the low-lying excited states of the BH molecule using the cc-pVDZ, cc-pVTZ, and cc-pVQZ basis sets. The LR-pCCD+S(HF) and LR-pCCD+S(pCCD) correspond to LR-pCCD+S calculations using canonical HF and variational orbital-optimized pCCD orbitals, respectively.

all excited states. We should stress here that this is not always the case for the augmented basis functions (see Figure S1 of the SI).

A statistical analysis of the LR-pCCD+S excited state properties is summarized in Table II. SD and MAE are the smallest for the LR-pCCD+S(HF) approach, indicating that, on average, the canonical HF orbitals provide a slightly better basis than the natural pCCD orbitals for LR-pCCD+S excited state properties (TDMs and OSs). This observation aligns with what has already been observed for pCCD-based electronic excitation energies, suggesting that the ground-state pCCD orbitals might not be optimal for excited-state calculations<sup>31</sup> (as to be expected). Notably, the OS, which depends directly on the excitation energy (cf. Eq. 25), shows no significant deviations from the statistical errors of TDMs. Table S5 of the SI dissects the statistical analysis by individual molecules and basis sets, providing a deeper look into their structure and basis set dependence. The largest statistical difference (SD and MAE) between the HF and pCCD bases is observed for the BH molecule.

In summary, by averaging over the basis sets and molecules summarized in Table S5, our in-depth compar-

ison of the LR-pCCD+S approaches to LR-CCSD indicates LR-pCCD+S(HF) as the most reliable method for modeling singly excited state properties of simple molecules (see Table II for statistics). Changing the canonical HF basis to the natural, symmetry-broken pCCD-optimized one increases errors (SD and MAE) from about 1 to 2%, while the MAE for the TDM is 3 to 5%.

TABLE II. Summary of statistical analysis of the LR-pCCD+S excited state properties w.r.t the LR-CCSD reference. SD(HF) and SD(pCCD) denote the standard deviation ( $SD = \sqrt{\frac{\sum_i^N (x_i^{\text{method}} - \bar{x})^2}{N}}$ ) using the canonical HF and the natural pCCD orbitals, respectively, while MAE indicates the mean absolute errors ( $MAE = \sum_i^N \frac{|x_i^{\text{method}} - x_i^{\text{ref}}|}{N}$ ) using HF and pCCD orbitals. The data corresponds to all molecules, excited states, and basis sets. See also Table S5 of the SI for statistical analysis for each individual basis set.

Property	SD (pCCD)	SD (HF)	MAE (pCCD)	MAE (HF)
TDM	0.0249	0.0156	0.0459	0.0327
OS	0.0111	0.0083	0.0210	0.0151

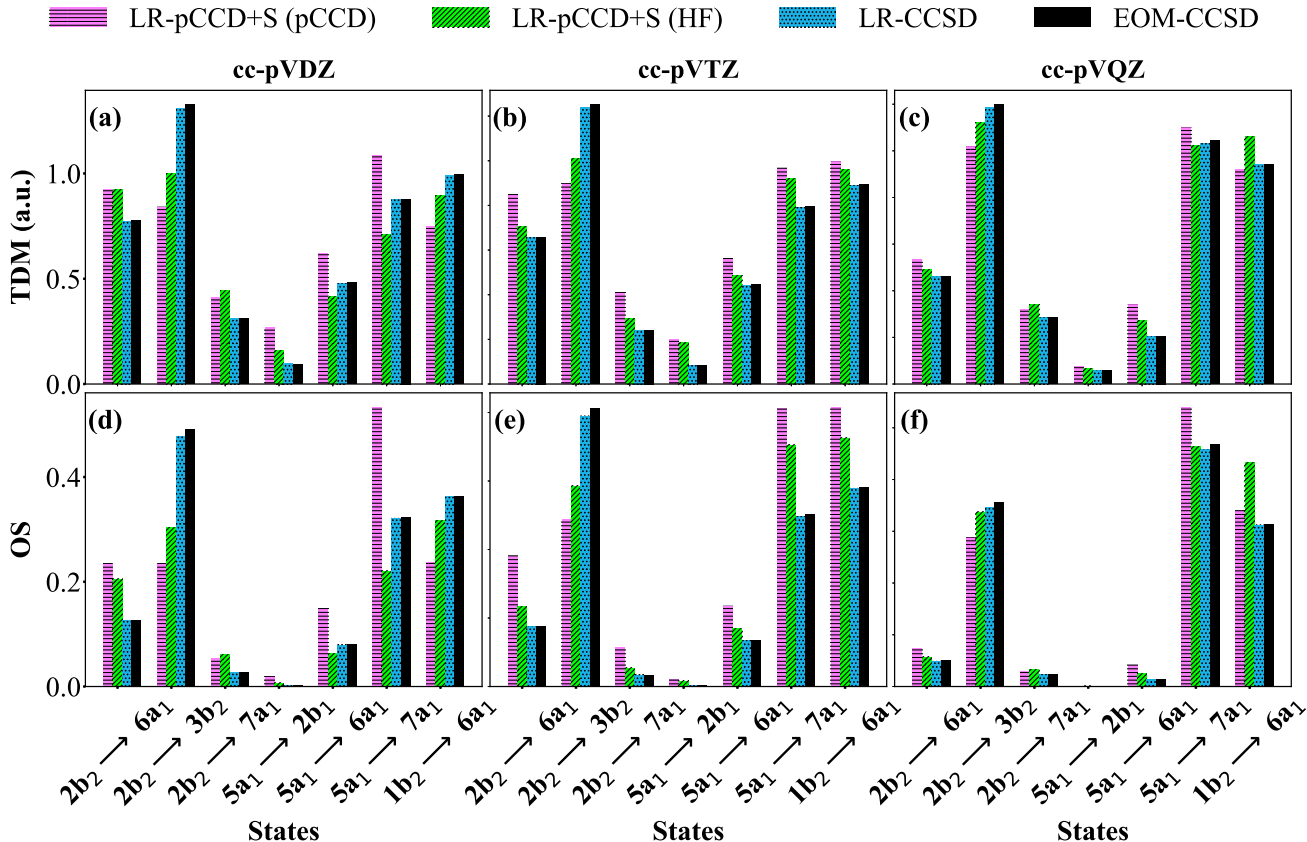


FIG. 2. LR-pCCD+S(HF), LR-pCCD+S(pCCD), LR-CCSD, and EOM-CCSD TDM and OS for the low-lying excited states of the  $\text{H}_2\text{CO}$  molecule using the cc-pVDZ, cc-pVTZ, and cc-pVQZ basis sets. The LR-pCCD+S(HF) and LR-pCCD+S(pCCD) correspond to LR-pCCD+S calculations using canonical HF and variational orbital-optimized pCCD orbitals, respectively.

## B. Double electron excitations

In the following, we focus on electronic excitations with a non-negligible double electron transfer character and their OSs. Specifically, we investigate the performance of the LR-pCCD+S methods in modeling the  $2^1A_1$  excited state of furan, cyclopentadiene, and pyridine. These are well-known, challenging examples for excited-state electronic structure methods. The CC2, CASSCF, and CC3 methods are often used to probe the percentage of double electron transfer in these systems.<sup>67</sup> As a reference for our LR-pCCD+S approaches, we use the CC3 method,<sup>68</sup> but we also report the CC2 results for comparison with our approach. We should stress, however, that the pure double-double excitation block of the CC2 Jacobian is only of zeroth order, meaning it is diagonal and consists solely of orbital energy differences. As a result, excitations dominated by singles are accurate up to the second order in CC2, whereas pure double excitations are accurate only to the zeroth order.<sup>67</sup> Also, similar to EOM-pCCD+S, LR-pCCD+S treats the double electronic transitions approximately, which are limited to the seniority zero sector.<sup>12</sup> Despite their questionable perfor-

mance for excited states with double excitation character, we will employ CC2 and CC3 as an indication measure for the presented LR-pCCD+S methods.

Our LR-pCCD+S results are summarized in Table III. Despite overestimating the excitation energies, LR-pCCD+S predicts oscillator strengths that agree well with the reference CC3 values for cyclopentadiene and pyridine. The only exception is the doubly excited state of the furan molecule. Most likely, this doubly excited state has non-negligible contributions from broken-pair excitations, as the LR-pCCD+S-based percentage contribution of  $R_2$  (more precisely,  $R_p$ ) is very low compared to other methods. Finally, similar to what we have observed earlier, the canonical HF orbital basis provides a more reliable description of LR-pCCD+S excited states and their properties than its pCCD counterpart.

## C. All-trans-polyenes

Finally, we move toward larger molecular structures to further validate our methods and investigate all-trans polyenes,  $\text{C}_{2n}\text{H}_{2n+2}$ , of different chain lengths with  $n =$

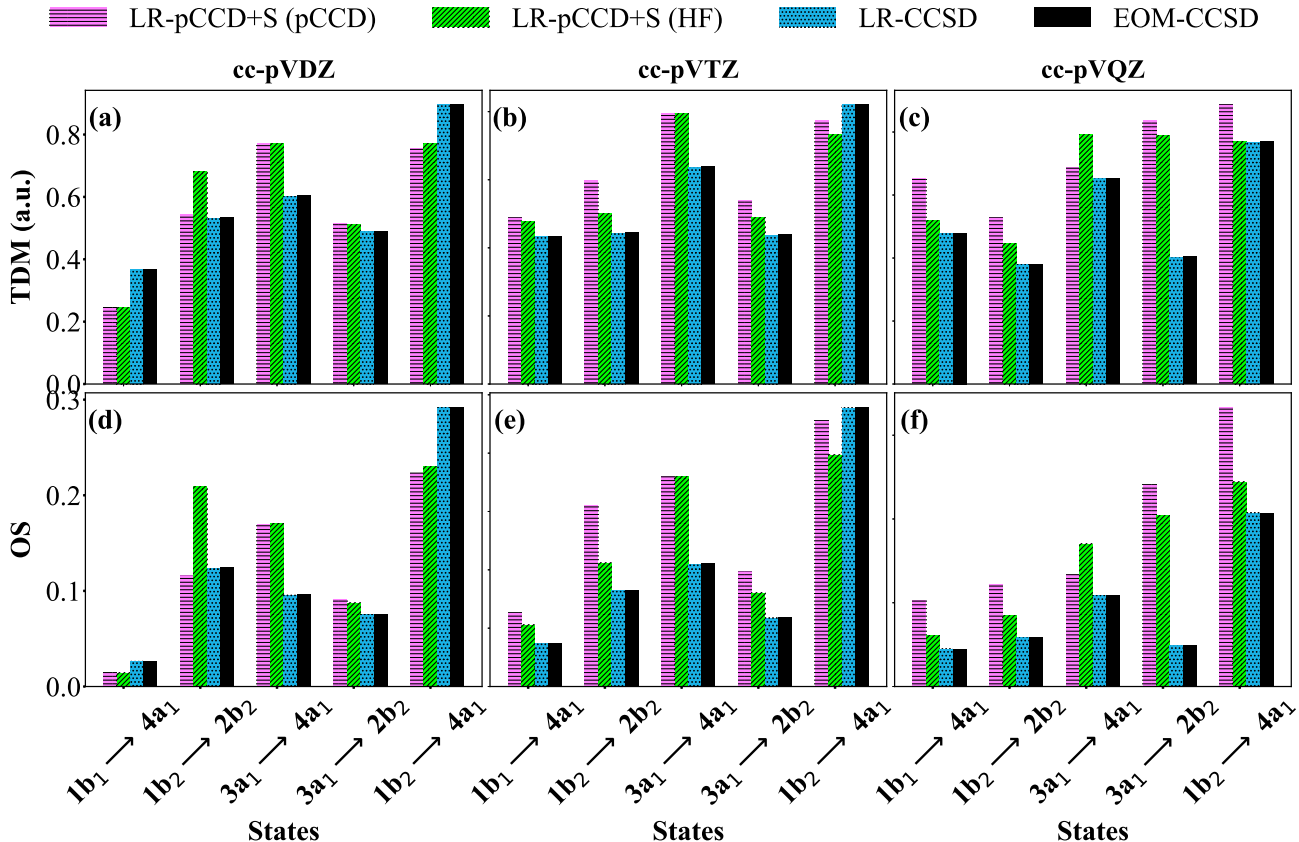


FIG. 3. LR-pCCD+S(HF), LR-pCCD+S(pCCD), LR-CCSD, and EOM-CCSD TDM and OS for the low-lying excited states of the  $\text{H}_2\text{O}$  molecule using the cc-pVDZ, cc-pVTZ, and cc-pVQZ basis sets. The LR-pCCD+S(HF) and LR-pCCD+S(pCCD) correspond to LR-pCCD+S calculations using canonical HF and variational orbital-optimized pCCD orbitals, respectively.

TABLE III. The  $2^1A_1$  ( $\pi \rightarrow \pi^*$ ) vertical excitation energies (EEs) and oscillator strengths (OSs) of furan, cyclopentadienyl, and pyridine using a def2-TZVP basis set. The values in parentheses represent the double excitation contributions ( $R_2$  or  $R_p$ ).

	Molecule	LR-pCCD+S(HF)	CC2 <sup>67</sup>	CC3 <sup>68</sup> ( $R_2$ <sup>69</sup> )
EE	Furan	7.95 (4%)	6.75	6.57 (16%)
	Cyclopentadiene	7.47 (56%)	7.05	6.28 (22%)
	Pyridine	6.44 (8%)	6.88	6.59 (7%)
OS	Furan	0.021	0.003	0.001
	Cyclopentadiene	0.004	0.011	0.005
	Pyridine	0.024	0.021	0.014

<sup>a</sup> Rate of the double excitations.

5, 6, 7, 8. Specifically, we focus on the  $1B_u^+$  state, which is known to have a non-negligible intensity and thus to be optically active. We used our LR-pCCD+S(HF) approach to determine the excitation energies and the corresponding OSs and TDMs. As previously reported,<sup>31,32</sup> EOM-pCCD+S(HF) provides reliable excitation energies for the lowest-lying  $B_u^+$  state in these challenging systems. In this work, we turn our attention toward the

corresponding excited state properties obtained from the proposed LR-pCCD-based models. To the best of our knowledge, the excited state properties of longer all-trans polyenes have not yet been studied with more elaborate ab initio methods.

Our results for the  $S_0$  structures are collected in Table IV. For longer chains, the oscillator strength follows a decreasing trend of excitation energies of the  $1B_u^+$  state. The TDMs and OSs reach their minima for the  $\text{C}_{14}\text{H}_{16}$  molecule. Since there is no other reliable theoretical data to verify our excited state properties, we compare our calculated excitation energies to the experimental spectra from Ref. 70. Similar to the trends in the oscillator strength predicted with LR-pCCD+S(HF), the experimental intensity decreases toward larger molecules (see Figure 2 of Ref. 70). Knowing that the LR-pCCD+S(HF) excited state properties are size intensive and the excitation energies of the  $1B_u^+$  state are reasonable (within the given basis set and molecular structures), we are quite confident that the results in Table IV are qualitatively correct.



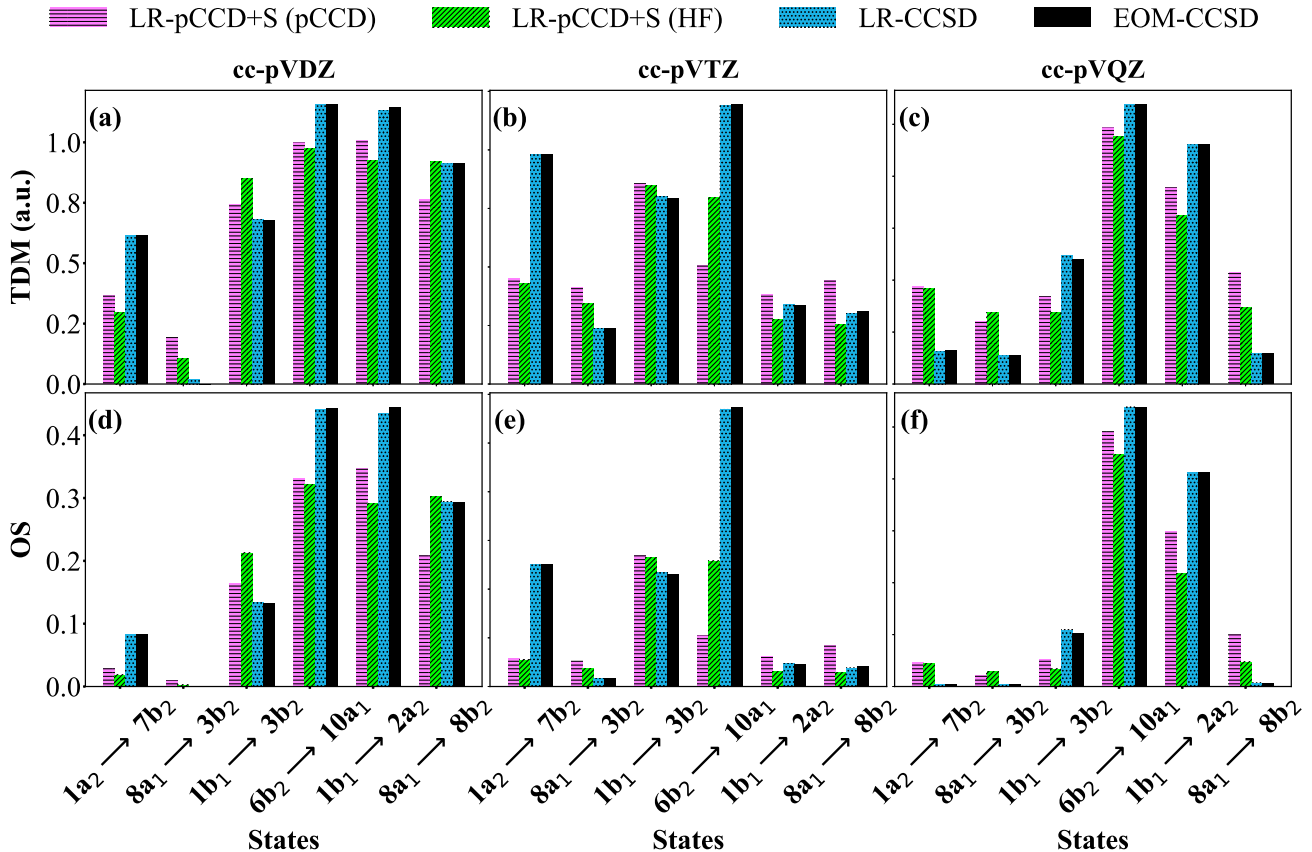


FIG. 4. LR-pCCD+S(HF), LR-pCCD+S(pCCD), LR-CCSD, and EOM-CCSD TDM and OS for the low-lying excited states of the furan ( $C_4H_4O$ ) molecule using the cc-pVDZ, cc-pVTZ, and cc-pVQZ basis sets. The LR-pCCD+S(HF) and LR-pCCD+S(pCCD) correspond to LR-pCCD+S calculations using canonical HF and variational orbital-optimized pCCD orbitals, respectively.

TABLE IV. LR-pCCD+S vertical excitation energies (EEs), oscillator strengths (OSs) and transition dipole moments (TDMs) for the  $B_u^+$  state in trans-polyenes.

Molecule	LR-pCCD+S(HF)			Exp. <sup>70</sup>
	EE (eV)	OS	TDM	EE (eV)
$C_{10}H_{12}$	4.91	2.56	0.88	4.60
$C_{12}H_{14}$	4.50	1.01	0.58	4.02
$C_{14}H_{16}$	4.25	1.00	0.59	3.74
$C_{16}H_{18}$	4.00	1.00	0.61	3.51

## V. CONCLUSIONS AND OUTLOOK

In this work, we derived the working equations for the LR-pCCD and LR-pCCD+S methods. While the first one has little use in quantum chemistry applications as it is restricted to pair excited states only, the latter provides a computationally inexpensive extension to the EOM-pCCD+S method,<sup>31,32</sup> allowing us to target excited state properties such as TDMs, OSs, and DSs (see SI) within the pCCD model, requiring only mean-field-like computational cost. Most importantly, our numerical exam-

ples validate the approximate inclusion of single excitations and the restriction to the right eigenstates only. Specifically, our study indicates a satisfyingly good performance of the LR-pCCD+S model for singly excited states, comparable to the LR-CCSD approach and the more expensive EOM-CCSD approach (mean-field-like vs.  $N^6$  scaling). Similar to EOM-pCCD+S excitation energies, excited state properties within the LR-pCCD+S framework are, on average, more reliable using canonical HF orbitals than the natural pCCD-optimized orbitals. Moreover, we demonstrate that our LR-pCCD+S(HF) method can also be used to predict excited state properties of more complex systems with a significant amount of double/bi-excitation character. Our LR-pCCD+S predictions are, however, limited to doubly excited states of seniority zero character. Finally, we provide a first theoretical description of electronic TDMs and OSs for the 1  $B_u^+$  state of longer all-trans polyene chains. Specifically, LR-pCCD+S(HF) predicts electronic properties in good agreement with experimentally recorded spectra.

In summary, we introduced a new cost-effective computational protocol representing a robust model to pre-

dict excited state properties qualitatively. To reduce the errors with respect to more elaborate models and hence to reach a more quantitative level for the prediction of excited state properties, we must account for the missing dynamic correlation energy in our LR-pCCD+S approach. Promising alternatives are various tailored coupled cluster corrections on top of the pCCD reference function<sup>12,19,23</sup> within the linear response framework. Finally, the pCCD-based transition density matrices open new ways to construct excited states' descriptors and topological analyses of charge transfer excited states<sup>71</sup> that are of great importance in organic electronics.<sup>25,72</sup>

## CONFLICTS OF INTEREST

There are no conflicts to declare.

## VI. ACKNOWLEDGEMENT

S. A. and P. T. acknowledge financial support from the SONATA BIS research grant from the National Science Centre, Poland (Grant No. 2021/42/E/ST4/00302). Funded/Co-funded by the European Union (ERC, DRESSED-pCCD, 101077420). Views and opinions expressed are, however, those of the author(s) only and do not necessarily reflect those of the European Union or the European Research Council. Neither the European Union nor the granting authority can be held responsible for them. S. A. gratefully acknowledges Prof. Iulia Emilia Brumboiu for the very helpful discussions.

## VII. SUPPINFO

Tables of data for TDM and OS, and DS results from Molpro and LR-pCCD+S in HF and pCCD base calculations for BH, H<sub>2</sub>O, H<sub>2</sub>CO, and furan molecules across different basis sets. Tables of statistical calculations for SD and MAE for individual molecules in various basis sets. A detailed explanation of the calculations used to obtain the final relation for transition matrix elements, including the vectors and matrices referenced in Table I.

## DATA AVAILABILITY STATEMENTS

The data underlying this study are available in the published article and its Supporting Information. The released version of the PyBEST code is available on Zenodo at <https://zenodo.org/records/10069179> and on PyPI at <https://pypi.org/project/pybest/>.

<sup>1</sup>A. D. Baker, C. R. Brundle, and M. Thompson, "Electron spectroscopy," *Chem. Soc. Rev.* **1**, 355–380 (1972).

<sup>2</sup>D. C. Harris and M. D. Bertolucci, *Symmetry and spectroscopy. An introduction to vibrational and electronic spectroscopy*. (Dover, 1989).

- <sup>3</sup>R. J. Bartlett, "Coupled-cluster approach to molecular structure and spectra: a step toward predictive quantum chemistry," *J. Chem. Phys.* **93**, 1697–1708 (1989).
- <sup>4</sup>A. Dreuw and M. Head-Gordon, "Single-reference ab initio methods for the calculation of excited states of large molecules," *Chem. Rev.* **105**, 4009–4037 (2005).
- <sup>5</sup>A. D. Becke, "Perspective: Fifty years of density-functional theory in chemical physics," *J. Chem. Phys.* **140**, 18A301 (2014).
- <sup>6</sup>M. Barbatti, A. J. Aquino, and H. Lischka, "The uv absorption of nucleobases: semi-classical ab initio spectra simulations," *Phys. Chem. Chem. Phys.* **12**, 4959–4967 (2010).
- <sup>7</sup>P. Tecmer, N. Govind, K. Kowalski, W. A. de Jong, and L. Visscher, "Reliable Modeling of the Electronic Spectra of Realistic Uranium Complexes," *J. Chem. Phys.* **139**, 034301 (2013).
- <sup>8</sup>E. Fromager, S. Knecht, and H. J. A. Jensen, "Multi-configuration time-dependent density-functional theory based on range separation," *J. Chem. Phys.* **138**, 084101 (2013).
- <sup>9</sup>R. J. Bartlett and M. Musiał, "Coupled-cluster theory in quantum chemistry," *Rev. Mod. Phys.* **79**, 291–350 (2007).
- <sup>10</sup>K. Raghavachari, G. W. Trucks, J. A. Pople, and M. Head-Gordon, "A fifth-order perturbation comparison of electron correlation theories," *Chem. Phys. Lett.* **157**, 479–483 (1989).
- <sup>11</sup>P. A. Limacher, P. W. Ayers, P. A. Johnson, S. De Baerdemacker, D. Van Neck, and P. Bultinck, "A new mean-field method suitable for strongly correlated electrons: computationally facile antisymmetric products of nonorthogonal geminals," *J. Chem. Theory Comput.* **9**, 1394–1401 (2013).
- <sup>12</sup>T. Stein, T. M. Henderson, and G. E. Scuseria, "Seniority zero pair coupled cluster doubles theory," *J. Chem. Phys.* **140**, 214113 (2014).
- <sup>13</sup>P. Tecmer and K. Boguslawski, "Geminal-based electronic structure methods in quantum chemistry. Toward geminal model chemistry," *Phys. Chem. Chem. Phys.* **24**, 23026–23048 (2022).
- <sup>14</sup>K. Boguslawski, P. Tecmer, P. W. Ayers, P. Bultinck, S. De Baerdemacker, and D. Van Neck, "Efficient description of strongly correlated electrons," *Phys. Rev. B* **89**, 201106(R) (2014).
- <sup>15</sup>P. A. Limacher, T. D. Kim, P. W. Ayers, P. A. Johnson, S. De Baerdemacker, D. Van Neck, and P. Bultinck, "The influence of orbital rotation on the energy of closed-shell wavefunctions," *Mol. Phys.* **112**, 853–862 (2014).
- <sup>16</sup>K. Boguslawski, P. Tecmer, P. A. Limacher, P. A. Johnson, P. W. Ayers, P. Bultinck, S. De Baerdemacker, and D. Van Neck, "Projected seniority-two orbital optimization of the antisymmetric product of one-reference orbital geminal," *J. Chem. Phys.* **140**, 214114 (2014).
- <sup>17</sup>K. Boguslawski, P. Tecmer, P. W. Ayers, P. Bultinck, S. De Baerdemacker, and D. Van Neck, "Non-variational orbital optimization techniques for the AP1roG wave function," *J. Chem. Theory Comput.* **10**, 4873–4882 (2014).
- <sup>18</sup>P. Limacher, P. Ayers, P. Johnson, S. De Baerdemacker, D. Van Neck, and P. Bultinck, "Simple and inexpensive perturbative correction schemes for antisymmetric products of nonorthogonal geminals," *Phys. Chem. Chem. Phys.* **16**, 5061–5065 (2014).
- <sup>19</sup>K. Boguslawski and P. W. Ayers, "Linearized coupled cluster correction on the antisymmetric product of 1-reference orbital geminals," *J. Chem. Theory Comput.* **11**, 5252–5261 (2015).
- <sup>20</sup>K. Boguslawski and P. Tecmer, "Benchmark of dynamic electron correlation models for seniority-zero wavefunctions and their application to thermochemistry," *J. Chem. Theory Comput.* **13**, 5966–5983 (2017).
- <sup>21</sup>A. Nowak and K. Boguslawski, "A configuration interaction correction on top of pair coupled cluster doubles," *Phys. Chem. Chem. Phys.* **25**, 7289–7301 (2023).
- <sup>22</sup>A. J. Garza, I. W. Bulik, T. M. Henderson, and G. E. Scuseria, "Range separated hybrids of pair coupled cluster doubles and density functionals," *Phys. Chem. Chem. Phys.* **17**, 22412–22422 (2015).
- <sup>23</sup>A. Leszczyk, M. Máté, Ó. Legeza, and K. Boguslawski, "Assessing the accuracy of tailored coupled cluster methods corrected

- by electronic wave functions of polynomial cost,” *J. Chem. Theory Comput.* **18**, 96–117 (2022).
- <sup>24</sup>K. Boguslawski, A. Leszczyk, A. Nowak, F. Brzęk, P. S. Żuchowski, D. Kędziera, and P. Tecmer, “Pythonic black-box electronic structure tool (PyBEST): an open-source python platform for electronic structure calculations at the interface between chemistry and physics,” *Comput. Phys. Commun.* **264**, 107933 (2021).
- <sup>25</sup>P. Tecmer, M. Gałyńska, L. Szczuczko, and K. Boguslawski, “Geminal-based strategies for modeling large building blocks of organic electronic materials,” *J. Phys. Chem. Lett.* **14**, 9909–9917 (2023).
- <sup>26</sup>M. Gałyńska, M. M. F. de Moraes, P. Tecmer, and K. Boguslawski, “Delving into the catalytic mechanism of molybdenum cofactors: A novel coupled cluster study,” *Phys. Chem. Chem. Phys.* **26**, 18918–18929 (2024).
- <sup>27</sup>M. H. Kriebel, P. Tecmer, M. Gałyńska, A. Leszczyk, and K. Boguslawski, “Accelerating Pythonic coupled cluster implementations: a comparison between CPUs and GPUs,” *J. Chem. Theory Comput.* **24**, 1130–1142 (2024).
- <sup>28</sup>D. J. Rowe, “Equations-of-motion method and the extended shell model,” *Rev. Mod. Phys.* **40**, 153–166 (1968).
- <sup>29</sup>J. F. Stanton and R. J. Bartlett, “The equation of motion coupled-cluster method. A systematic biorthogonal approach to molecular excitation energies, transition probabilities, and excited state properties,” *J. Chem. Phys.* **98**, 7029–7039 (1993).
- <sup>30</sup>R. J. Bartlett, “Coupled-cluster theory and its equation-of-motion extensions,” *WIREs Comput. Mol. Sci.* **2**, 126–138 (2012).
- <sup>31</sup>K. Boguslawski, “Targeting excited states in all-trans polyenes with electron-pair states,” *J. Chem. Phys.* **145**, 234105 (2016).
- <sup>32</sup>K. Boguslawski, “Erratum: “Targeting excited states in all-trans polyenes with electron-pair states,”” *J. Chem. Phys.* **147**, 139901 (2017).
- <sup>33</sup>K. Boguslawski, “Targeting doubly excited states with equation of motion coupled cluster theory restricted to double excitations,” *J. Chem. Theory Comput.* **15**, 18–24 (2019).
- <sup>34</sup>S. Jahani, K. Boguslawski, and P. Tecmer, “The relationship between structure and excited-state properties in polyanilines from geminal-based methods,” *RSC Adv.* **13**, 27898–27911 (2023).
- <sup>35</sup>H. Sekino and R. J. Bartlett, “A linear response, coupled-cluster theory for excitation energy,” *Int. J. Quantum Chem.* **26**, 255–265 (1984).
- <sup>36</sup>H. Koch and P. Jørgensen, “Coupled cluster response functions,” *J. Chem. Phys.* **93**, 3333–3344 (1990).
- <sup>37</sup>H. Koch, H. J. A. Jensen, P. Jørgensen, and T. Helgaker, “Excitation energies from the coupled cluster singles and doubles linear response function (ccsdlr). applications to be, ch<sup>+</sup>, co, and H<sub>2</sub>O,” *J. Chem. Phys.* **93**, 3345–3350 (1990).
- <sup>38</sup>O. Christiansen, P. Jørgensen, and C. Hättig, “Response functions from fourier component variational perturbation theory applied to a time-averaged quasienergy,” *Int. J. Quantum Chem.* **68**, 1–52 (1998).
- <sup>39</sup>J. D. Watts, “An introduction to equation-of-motion and linear-response coupled-cluster methods for electronically excited states of molecules,” in *Radiation Induced Molecular Phenomena in Nucleic Acids* (Springer, 2008) pp. 65–92.
- <sup>40</sup>H. Koch, R. Kobayashi, A. Sanchez de Merás, and P. Jørgensen, “Calculation of size-intensive transition moments from the coupled cluster singles and doubles linear response function,” *J. Chem. Phys.* **100**, 4393–4400 (1994).
- <sup>41</sup>K. Hald, C. Hättig, J. Olsen, and P. Jørgensen, “CC3 triplet excitation energies using an explicit spin coupled excitation space,” *J. Chem. Phys.* **115**, 3545–3552 (2001).
- <sup>42</sup>O. Christiansen, H. Koch, and P. Jørgensen, “Perturbative triple excitation corrections to coupled cluster singles and doubles excitation energies,” *J. Chem. Phys.* **105**, 1451–1459 (1996).
- <sup>43</sup>O. Christiansen, H. Koch, P. Jørgensen, and J. Olsen, “Excitation energies of h<sub>2</sub>o, n<sub>2</sub> and c<sub>2</sub> in full configuration interaction and coupled cluster theory,” *Chem. Phys. Lett.* **256**, 185–194 (1996).
- <sup>44</sup>A. Nowak, P. Tecmer, and K. Boguslawski, “Assessing the accuracy of simplified coupled cluster methods for electronic excited states in f0 actinide compounds,” *Phys. Chem. Chem. Phys.* **21**, 19039–19053 (2019).
- <sup>45</sup>J. Čížek, “On the correlation problem in atomic and molecular systems. calculation of wavefunction components in urself-type expansion using quantum-field theoretical methods,” *J. Chem. Phys.* **45**, 4256–4266 (1966).
- <sup>46</sup>J. Čížek and J. Paldus, “Correlation problems in atomic and molecular systems iii. rederivation of the coupled-pair many-electron theory using the traditional quantum chemical methods,” *Int. J. Quantum Chem.* **5**, 359–379 (1971).
- <sup>47</sup>P. Tecmer, A. S. P. Gomes, S. Knecht, and L. Visscher, “Communication: Relativistic Fock-Space Coupled Cluster Study of Small Building Blocks of Larger Uranium Complexes,” *J. Chem. Phys.* **141**, 041107 (2014).
- <sup>48</sup>F. Brzęk, K. Boguslawski, P. Tecmer, and P. S. Żuchowski, “Benchmarking the accuracy of seniority-zero wave function methods for noncovalent interactions,” *J. Chem. Theory Comput.* **15**, 4021–4035 (2019).
- <sup>49</sup>J. Olsen and P. Jørgensen, “Linear and nonlinear response functions for an exact state and for an mscf state,” *J. Chem. Phys.* **82**, 3235–3264 (1985).
- <sup>50</sup>H. Koch, H. J. Jensen, T. Helgaker, G. E. Scuseria, and H. F. Schaefer, “Coupled cluster energy derivatives. analytic hessian for the closed-shell coupled cluster singles and doubles wave function: Theory and applications,” *J. Chem. Phys.* **92**, 4924–4940 (1990).
- <sup>51</sup>P. Jørgensen and T. Helgaker, “Møller–plesset energy derivatives,” *J. Chem. Phys.* **89**, 1560–1570 (1988).
- <sup>52</sup>R. J. Cave and E. R. Davidson, “A theoretical investigation of some low-lying singlet states of 1, 3-butadiene,” *J. Chem. Phys.* **91**, 4481–4490 (1987).
- <sup>53</sup>T. B. Pedersen, A. M. Sánchez de Merás, and H. Koch, “Polarizability and optical rotation calculated from the approximate coupled cluster singles and doubles cc2 linear response theory using cholesky decompositions,” *J. Chem. Phys.* **120**, 8887–8897 (2004).
- <sup>54</sup>A. M. Tucholska, M. Modrzejewski, and R. Moczyński, “Transition properties from the hermitian formulation of the coupled cluster polarization propagator,” *J. Chem. Phys.* **141** (2014).
- <sup>55</sup>K. Boguslawski, F. Brzęk, R. Chakraborty, K. Cieślak, S. Jahani, A. Leszczyk, A. Nowak, E. Sujkowski, J. Świerczyński, S. Ahmadvani, D. Kędziera, M. H. Kriebel, P. S. Żuchowski, and P. Tecmer, “Pybest: improved functionality and enhanced performance,” *Comput. Phys. Commun.* **297**, 109049 (2024).
- <sup>56</sup>A. Chrayteh, A. Blondel, P.-F. Loos, and D. Jacquemin, “Mountaineering strategy to excited states: highly accurate oscillator strengths and dipole moments of small molecules,” *J. Chem. Theory Comput.* **17**, 416–438 (2020).
- <sup>57</sup>P.-F. Loos, F. Lipparini, M. Boggio-Pasqua, A. Scemama, and D. Jacquemin, “A mountaineering strategy to excited states: Highly accurate energies and benchmarks for medium sized molecules,” *J. Chem. Theory Comput.* **16**, 1711–1741 (2020).
- <sup>58</sup>T. Dunning Jr., “Gaussian basis sets for use in correlated molecular calculations. I. The atoms boron through neon and hydrogen,” *J. Chem. Phys.* **90**, 1007–1023 (1989).
- <sup>59</sup>R. A. Kendall, T. H. Dunning, and R. J. Harrison, “Electron affinities of the 1st-row atoms revisited - systematic basis-sets and wave-functions,” *J. Chem. Phys.* **96**, 6796 (1989).
- <sup>60</sup>F. Weigend and R. Ahlrichs, “Balanced basis sets of split valence, triple zeta valence and quadruple zeta valence quality for H to Rn: Design and assessment of accuracy,” *Phys. Chem. Chem. Phys.* **7**, 3297–3305 (2005).
- <sup>61</sup>W. Hu and G. K.-L. Chan, “Excited-State Geometry Optimization with the Density Matrix Renormalization Group, as Applied to Polyenes,” *J. Chem. Theory Comput.* **11**, 3000–3009 (2015).
- <sup>62</sup>H.-J. Werner, P. J. Knowles, P. Celani, W. Györfy, A. Hesselmann, D. Kats, G. Knizia, A. Köhn, T. Korona, D. Kreplin, R. Lindh, Q. Ma, F. R. Manby, A. Mitrushenkov, G. Rauhut,

- M. Schütz, K. R. Shamasundar, T. B. Adler, R. D. Amos, S. J. Bennie, A. Bernhardsson, A. Berning, J. A. Black, P. J. Bygrave, R. Cimiraglia, D. L. Cooper, D. Coughtrie, M. J. O. Deegan, A. J. Dobbyn, K. Doll, M. Dornbach, F. Eckert, S. Erfort, E. Goll, C. Hampel, G. Hetzer, J. G. Hill, M. Hodges, T. Hrenar, G. Jansen, C. Köppl, C. Kollmar, S. J. R. Lee, Y. Liu, A. W. Lloyd, R. A. Mata, A. J. May, B. Mussard, S. J. McNicholas, W. Meyer, T. F. Miller III, M. E. Mura, A. Nicklass, D. P. O'Neill, P. Palmieri, D. Peng, K. A. Peterson, K. Pflüger, R. Pitzer, I. Polyak, M. Reiher, J. O. Richardson, J. B. Robinson, B. Schröder, M. Schwilk, T. Shiozaki, M. Sibaev, H. Stoll, A. J. Stone, R. Tarroni, T. Thorsteinsson, J. Toulouse, M. Wang, M. Welborn, and B. Ziegler, "Molpro, version 2020.2.1, a package of *ab initio* programs," (2020), see <http://www.molpro.net> (accessed March 1, 2024).
- <sup>63</sup>H.-J. W. Werner, J. P. Knowles, F. R. Manby, J. A. Black, K. Doll, A. Heßelmann, D. Kats, A. Köhn, T. Korona, D. A. Kreplin, Q. Ma, T. F. Miller III, A. Mitrushchenkov, K. A. Peterson, I. Polyak, G. Rauhut, and M. Sibaev, "The Molpro quantum chemistry package," *J. Chem. Phys.* **152**, 144107 (2020).
- <sup>64</sup>H.-J. Werner, J. P. Knowles, G. Knizia, F. R. Manby, and M. Schütz, "Molpro: A General Purpose Quantum Chemistry Program Package," *WIREs Comput. Mol. Sci.* **2**, 242–253 (2012).
- <sup>65</sup>K. Aidas, C. Angeli, K. L. Bak, V. Bakken, R. Bast, L. Boman, O. Christiansen, R. Cimiraglia, S. Coriani, P. Dahle, E. K. Dalskov, U. Ekström, T. Enevoldsen, J. J. Eriksen, P. Ettenhuber, B. Fernández, L. Ferrighi, H. Fliegl, L. Frediani, K. Hald, A. Halkier, C. Hättig, H. Heiberg, T. Helgaker, A. C. Hennum, H. Hettema, E. Hjertenes, S. Høst, I.-M. Høyvik, M. F. Iozzi, B. Jansík, H. J. A. Jensen, D. Jonsson, P. Jørgensen, J. Kauczor, S. Kirpekar, T. Kjærgaard, W. Klopper, S. Knecht, R. Kobayashi, H. Koch, J. Kongsted, A. Krapp, K. Kristensen, A. Ligabue, O. B. Lutnæs, J. I. Melo, K. V. Mikkelsen, R. H. Myhre, C. Neiss, C. B. Nielsen, P. Norman, J. Olsen, J. M. H. Olsen, A. Osted, M. J. Packer, F. Pawłowski, T. B. Pedersen, P. F. Provasi, S. Reine, Z. Rinkevicius, T. A. Ruden, K. Ruud, V. V. Rybkin, P. Salek, C. C. M. Samson, A. S. de Merás, T. Saue, S. P. A. Sauer, B. Schimmelpfennig, K. Sneskov, A. H. Steindal, K. O. Sylvester-Hvid, P. R. Taylor, A. M. Teale, E. I. Tellgren, D. P. Tew, A. J. Thorvaldsen, L. Thøgersen, O. Vahtras, M. A. Watson, D. J. D. Wilson, M. Ziolkowski, and H. Ågren, "The dalton quantum chemistry program system," *WIREs Comput. Mol. Sci.* **4**, 269–284 (2013).
- <sup>66</sup>Dalton, a molecular electronic structure program, Release v2020.0 (2020), see <http://daltonprogram.org>.
- <sup>67</sup>M. Schreiber, M. R. Silva-Junior, S. P. A. Sauer, and W. Thiel, "Benchmarks for electronically excited states: Caspt2, cc2, ccSD, and cc3," *J. Chem. Phys.* **128**, 134110 (2008).
- <sup>68</sup>S. P. A. Sauer, H. F. Pitzner-Frydendahl, M. Buse, H. J. A. Jensen, and W. Thiel, "Performance of soppa-based methods in the calculation of vertical excitation energies and oscillator strengths," *Mol. Phys.* **113**, 2026–2045 (2015).
- <sup>69</sup>S. P. A. Sauer, M. Schreiber, M. R. Silva-Junior, and W. Thiel, "Benchmarks for electronically excited states: a comparison of noniterative and iterative triples corrections in linear response coupled cluster methods: Ccsdr(3) versus cc3," *J. Chem. Theory Comput.* **5**, 555–564 (2009).
- <sup>70</sup>R. L. Christensen, M. G. I. Galinato, E. F. Chu, J. N. Howard, R. D. Broene, and H. A. Frank, "Energies of low-lying excited states of linear polyenes," *J. Phys. Chem. A* **112**, 12629–12636 (2008).
- <sup>71</sup>T. Etienne, "Transition matrices and orbitals from reduced density matrix theory," *J. Chem. Phys.* **142**, 244103 (2015).
- <sup>72</sup>F. Labat, T. Le Bahers, I. Ciofini, and C. Adamo, "First-principles modeling of dye-sensitized solar cells: challenges and perspectives," *Acc. Chem. Res.* **45**, 1268–1277 (2012).

# Linear response pCCD-based methods: LR-pCCD and LR-pCCD+S approaches for the efficient and reliable modelling of excited state properties

Somayeh Ahmadkhani<sup>†</sup>, Katharina Boguslawski, and Paweł Tecmer<sup>†</sup>

Institute of Physics, Faculty of Physics, Astronomy, and Informatics, Nicolaus Copernicus University in Toruń, Grudziadzka 5, Toruń, 87-100 Toruń, Poland

<sup>†</sup>E-mail:so.ahmadkhani@gmail.com; ptecmer@fizyka.umk.pl

**Supplementary Information**

**S1 Numerical results for single excitation energies.**

Table S1: Vertical excitation energies (EE), TDMs, DSs, and OSs for H<sub>2</sub>CO in ground state geometry using cc-pVDZ, cc-pVTZ, cc-pVQZ and aug-cc-pVTZ basis sets.

		cc-pVDZ						
Property	Method	2b <sub>2</sub> → 6a <sub>1</sub>	2b <sub>2</sub> → 3b <sub>2</sub>	2b <sub>2</sub> → 7a <sub>1</sub>	5a <sub>1</sub> → 2b <sub>1</sub>	5a <sub>1</sub> → 6a <sub>1</sub>	5a <sub>1</sub> → 7a <sub>1</sub>	1b <sub>2</sub> → 6a <sub>1</sub>
EE	LR-pCCDS(pCCD)	0.4121	0.4999	0.4817	0.4160	0.5826	0.6829	0.6371
	LR-pCCDS(HF)	0.3626	0.4570	0.4655	0.3934	0.5594	0.6599	0.5932
	LR-CCSD	0.3177	0.4183	0.4260	0.3490	0.5231	0.6288	0.5540
	EOM-CCSD	0.3177	0.4183	0.4260	0.3490	0.5231	0.6288	0.5540
	CCSDR(3)	0.3149	0.4132	0.4263	0.3467	0.5169	0.6264	0.5467
TDM	LR-pCCDS(pCCD)	0.9231	0.8408	0.4105	0.2665	0.6217	1.0831	0.7478
	LR-pCCDS(HF)	0.9234	0.9999	0.4455	0.1609	0.4136	0.7089	0.8966
	LR-CCSD	0.7716	1.3105	0.3095	0.0975	0.4783	0.8766	0.9925
	EOM-CCSD	0.7747	1.3283	0.3106	0.0927	0.4825	0.8787	0.9929
DS	LR-pCCDS(pCCD)	0.8521	0.7069	0.1685	0.0710	0.3865	1.1732	0.5592
	LR-pCCDS(HF)	0.8526	0.9998	0.1985	0.0259	0.1711	0.5026	0.8039
	LR-CCSD	0.5954	1.7173	0.0958	0.0095	0.2288	0.7684	0.9850
	EOM-CCSD	0.6001	1.7643	0.0965	0.0086	0.2328	0.7722	0.9858
OS	LR-pCCDS(pCCD)	0.2341	0.2356	0.0541	0.0197	0.1501	0.5341	0.2375
	LR-pCCDS(HF)	0.2061	0.3046	0.0616	0.0068	0.0638	0.2211	0.3179
	LR-CCSD	0.1261	0.4789	0.0272	0.0022	0.0798	0.3221	0.3638
	EOM-CCSD	0.1271	0.4920	0.0274	0.0020	0.0812	0.3237	0.3641
		cc-pVTZ						
		2b <sub>2</sub> → 6a <sub>1</sub>	2b <sub>2</sub> → 3b <sub>2</sub>	2b <sub>2</sub> → 7a <sub>1</sub>	5a <sub>1</sub> → 2b <sub>1</sub>	5a <sub>1</sub> → 6a <sub>1</sub>	5a <sub>1</sub> → 7a <sub>1</sub>	1b <sub>2</sub> → 6a <sub>1</sub>
EE	LR-pCCDS(pCCD)	0.3988	0.4551	0.5090	0.4037	0.5620	0.6510	0.6176
	LR-pCCDS(HF)	0.3515	0.4309	0.4783	0.3715	0.5363	0.6268	0.5888
	LR-CCSD	0.3065	0.3881	0.4408	0.3435	0.5180	0.5983	0.5508
	EOM-CCSD	0.3065	0.3881	0.4408	0.3435	0.5180	0.5983	0.5508
	CCSDR(3)	0.3025	0.3829	0.4366	0.3406	0.5146	0.5933	0.5450
TDM	LR-pCCDS(pCCD)	0.8467	0.8972	0.4116	0.2012	0.5617	0.9677	0.9958
	LR-pCCDS(HF)	0.7069	1.0101	0.2943	0.1873	0.4870	0.9186	0.9615
	LR-CCSD	0.6563	1.2365	0.2419	0.0837	0.4422	0.7892	0.8885
	EOM-CCSD	0.6585	1.2528	0.2419	0.0837	0.4441	0.7947	0.8916
DS	LR-pCCDS(pCCD)	0.7169	0.8049	0.1694	0.0405	0.3155	0.9364	0.9917
	LR-pCCDS(HF)	0.4997	1.0203	0.0866	0.0351	0.2372	0.8438	0.9245
	LR-CCSD	0.4307	1.5290	0.0585	0.0070	0.1955	0.6228	0.7895
	EOM-CCSD	0.4336	1.5696	0.0585	0.0070	0.1972	0.6315	0.7949
OS	LR-pCCDS(pCCD)	0.1906	0.2442	0.0575	0.0109	0.1182	0.4064	0.4083
	LR-pCCDS(HF)	0.1171	0.2931	0.0276	0.0087	0.0848	0.3526	0.3629
	LR-CCSD	0.0880	0.3956	0.0172	0.0016	0.0675	0.2484	0.2899
	EOM-CCSD	0.0886	0.4061	0.0172	0.0016	0.0681	0.2519	0.2919
		cc-pVQZ						
		2b <sub>2</sub> → 6a <sub>1</sub>	2b <sub>2</sub> → 3b <sub>2</sub>	2b <sub>2</sub> → 7a <sub>1</sub>	5a <sub>1</sub> → 2b <sub>1</sub>	5a <sub>1</sub> → 6a <sub>1</sub>	5a <sub>1</sub> → 7a <sub>1</sub>	1b <sub>2</sub> → 6a <sub>1</sub>
EE	LR-pCCDS(pCCD)	0.3861	0.4171	0.4518	0.4006	0.5395	0.6680	0.6022
	LR-pCCDS(HF)	0.3568	0.4039	0.4383	0.3835	0.5130	0.6642	0.5755
	LR-CCSD	0.3529	0.3722	0.4326	0.3426	0.4992	0.6455	0.5307
	EOM-CCSD	0.3529	0.3722	0.4326	0.3426	0.4992	0.6455	0.5307
	CCSDR(3)	0.3507	0.3665	0.4284	0.3394	0.4923	0.6385	0.5223
TDM	LR-pCCDS(pCCD)	0.5351	1.0182	0.3187	0.0748	0.3404	1.1017	0.9212
	LR-pCCDS(HF)	0.4904	1.1196	0.3391	0.0656	0.2726	1.0242	1.0633
	LR-CCSD	0.4610	1.1839	0.2855	0.0592	0.2052	1.0316	0.9398
	EOM-CCSD	0.4628	1.1995	0.2860	0.0592	0.2059	1.0433	0.9412
DS	LR-pCCDS(pCCD)	0.2863	1.0368	0.1016	0.0056	0.1159	1.2137	0.8486
	LR-pCCDS(HF)	0.2405	1.2534	0.1150	0.0043	0.0743	1.0490	1.1307
	LR-CCSD	0.2125	1.4017	0.0815	0.0035	0.0421	1.0643	0.8833
	EOM-CCSD	0.2142	1.4387	0.0818	0.0035	0.0424	1.0885	0.8858
OS	LR-pCCDS(pCCD)	0.0737	0.2883	0.0306	0.0015	0.0417	0.5405	0.3407
	LR-pCCDS(HF)	0.0572	0.3375	0.0336	0.0011	0.0254	0.4645	0.4338
	LR-CCSD	0.0500	0.3478	0.0235	0.0008	0.0140	0.4580	0.3125
	EOM-CCSD	0.0504	0.3570	0.0236	0.0008	0.0141	0.4684	0.3134

		aug-cc-pVTZ						
Property	Method	$2b_2 \rightarrow 6a_1$	$2b_2 \rightarrow 3b_2$	$2b_2 \rightarrow 7a_1$	$5a_1 \rightarrow 2b_1$	$5a_1 \rightarrow 6a_1$	$5a_1 \rightarrow 7a_1$	$1b_2 \rightarrow 6a_1$
EE	LR-pCCDS(pCCD)	0.3477	0.3961	0.4499	0.3768	0.4150	0.5685	0.5555
	LR-pCCDS(HF)	0.3207	0.3583	0.4228	0.3507	0.4204	0.5619	0.5487
	LR-CCSD	0.2984	0.3554	0.4031	0.3411	0.3805	0.5377	0.3825
	EOM-CCSD	0.2984	0.3554	0.4031	0.3411	0.3805	0.5377	0.3825
	CCSDR(3)	0.2970	0.3495	0.4001	0.3381	0.3788	0.5283	0.3811
TDM	LR-pCCDS(pCCD)	0.4237	1.0166	0.6748	0.1828	0.2681	0.8889	0.7575
	LR-pCCDS(HF)	0.5182	1.2075	0.5809	0.0583	0.1400	0.4179	0.6158
	LR-CCSD	0.4478	0.7669	0.4050	0.0520	0.0100	0.2200	0.1997
	EOM-CCSD	0.4496	0.7780	0.4063	0.0548	0.0100	0.2205	0.2005
DS	LR-pCCDS(pCCD)	0.1795	1.0335	0.4554	0.0334	0.0719	0.7902	0.5738
	LR-pCCDS(HF)	0.2685	1.4581	0.3374	0.0034	0.0196	0.1746	0.3792
	LR-CCSD	0.2005	0.5881	0.1640	0.0027	0.0001	0.0484	0.0399
	EOM-CCSD	0.2021	0.6053	0.1651	0.0030	0.0001	0.0486	0.0402
OS	LR-pCCDS(pCCD)	0.0416	0.2729	0.1366	0.0084	0.0199	0.2995	0.2125
	LR-pCCDS(HF)	0.0574	0.3483	0.0951	0.0008	0.0055	0.0654	0.1387
	LR-CCSD	0.0399	0.1393	0.0441	0.0006	0.0000	0.0174	0.0102
	EOM-CCSD	0.0402	0.1434	0.0444	0.0007	0.0000	0.0174	0.0103



Table S2: Vertical excitation energies (EE), TDMs, DSs, and OSs for BH in ground state geometry using cc-pVDZ, cc-pVTZ, cc-pVQZ and aug-cc-pVTZ basis sets.

Property	Method	cc-pVDZ			cc-pVTZ		
		$3\sigma \rightarrow 1\pi$	$3\sigma \rightarrow 4\sigma$	$3\sigma \rightarrow 2\pi$	$3\sigma \rightarrow 1\pi$	$3\sigma \rightarrow 4\sigma$	$3\sigma \rightarrow 2\pi$
EE	LR-pCCD+S (pCCD)	0.1527	0.4052	0.4705	0.1563	0.3995	0.4467
	LR-pCCD+S (HF)	0.1089	0.3951	0.4550	0.1223	0.3559	0.3917
	LR-CCSD	0.1119	0.3683	0.3987	0.1089	0.3408	0.3803
	EOM-CCSD	0.1119	0.3683	0.3987	0.1086	0.3408	0.3803
	CCSDR(3)	0.1111	0.3673	0.3949	0.1076	0.3392	0.3772
TDM	LR-pCCD+S (pCCD)	0.6078	0.9645	0.9797	0.7989	1.0176	0.6437
	LR-pCCD+S (HF)	0.6188	0.9744	0.9239	0.6265	1.4256	0.8899
	LR-CCSD	0.6126	1.7061	1.0190	0.6019	1.5435	0.9233
	EOM-CCSD	0.6148	1.7058	1.0240	0.6061	1.5418	0.9279
DS	LR-pCCD+S (pCCD)	0.3694	0.9303	0.9599	0.6382	1.0355	0.4144
	LR-pCCD+S (HF)	0.3829	0.9495	0.8535	0.3925	2.0323	0.7919
	LR-CCSD	0.3753	2.9108	1.0384	0.3623	2.3825	0.8524
	EOM-CCSD	0.3780	2.9096	1.0485	0.3674	2.3772	0.8610
OS	LR-pCCD+S (pCCD)	0.0376	0.2513	0.3011	0.0665	0.2758	0.1234
	LR-pCCD+S (HF)	0.0278	0.2501	0.2589	0.0320	0.4822	0.2068
	LR-CCSD	0.0280	0.7147	0.2760	0.0263	0.5413	0.2161
	EOM-CCSD	0.0282	0.7144	0.2787	0.0266	0.5401	0.2183
		cc-pVQZ			aug-cc-pVTZ		
Property	Method	$3\sigma \rightarrow 1\pi$	$3\sigma \rightarrow 4\sigma$	$3\sigma \rightarrow 2\pi$	$3\sigma \rightarrow 1\pi$	$3\sigma \rightarrow 4\sigma$	$3\sigma \rightarrow 2\pi$
EE	LR-pCCD+S (pCCD)	0.1570	0.3769	0.4030	0.1590	0.2767	0.3150
	LR-pCCD+S (HF)	0.1197	0.3272	0.3708	0.1161	0.2447	0.2839
	LR-CCSD	0.1076	0.3046	0.3498	0.1075	0.2405	0.2808
	EOM-CCSD	0.1076	0.3046	0.3498	0.1075	0.2405	0.2808
	CCSDR(3)	0.1065	0.3028	0.3476	0.1052	0.2391	0.2796
TDM	LR-pCCD+S (pCCD)	0.7836	1.1245	0.4319	1.1948	2.034	0.564
	LR-pCCD+S (HF)	0.6742	1.1713	0.5545	2.3298	2.0032	0.7479
	LR-CCSD	0.5974	1.0092	0.6359	2.2403	2.0857	0.7135
	EOM-CCSD	0.6021	1.0065	0.6379	2.2272	2.0798	0.7142
DS	LR-pCCD+S (pCCD)	0.6140	1.2644	0.1865	1.4276	4.1371	0.3181
	LR-pCCD+S (HF)	0.4545	1.3720	0.3075	5.4279	4.0129	0.5593
	LR-CCSD	0.3569	1.0184	0.4044	5.0191	4.3503	0.5091
	EOM-CCSD	0.3625	1.0130	0.4069	4.9605	4.3254	0.5101
OS	LR-pCCD+S (pCCD)	0.0490	0.2758	0.0461	0.1105	0.6749	0.0602
	LR-pCCD+S (HF)	0.0326	0.2786	0.0717	0.3890	0.6434	0.1047
	LR-CCSD	0.0256	0.2068	0.0943	0.3597	0.6975	0.0953
	EOM-CCSD	0.0260	0.2057	0.0949	0.3555	0.6935	0.0955

Table S3: Vertical excitation energies (EE), TDMs, DSs, and OSs for H<sub>2</sub>O in ground state geometry using cc-pVDZ, cc-pVTZ, cc-pVQZ and aug-cc-pVTZ basis sets.

		cc-pVDZ				
Property	Method	1b <sub>1</sub> → 4a <sub>1</sub>	1b <sub>2</sub> → 2b <sub>2</sub>	3a <sub>1</sub> → 4a <sub>1</sub>	3a <sub>1</sub> → 2b <sub>2</sub>	1b <sub>2</sub> → 4a <sub>1</sub>
EE	LR-pCCD+S (pCCD)	0.3630	0.5908	0.4301	0.5131	0.5903
	LR-pCCD+S (HF)	0.3539	0.6751	0.4286	0.5036	0.5779
	LR-CCSD	0.3001	0.6584	0.3976	0.4746	0.5454
	EOM-CCSD	0.3001	0.6584	0.3976	0.4746	0.5454
	CCSDR(3)	0.3016	0.6571	0.3986	0.4753	0.5448
TDM	LR-pCCD+S (pCCD)	0.2447	0.5430	0.7700	0.5158	0.7729
	LR-pCCD+S (HF)	0.2454	0.6821	0.7727	0.5114	0.7728
	LR-CCSD	0.3661	0.5310	0.6018	0.4885	0.8963
	EOM-CCSD	0.3661	0.5330	0.6034	0.4898	0.8969
DS	LR-pCCD+S (pCCD)	0.0599	0.2948	0.5929	0.2660	0.5974
	LR-pCCD+S (HF)	0.0602	0.4653	0.5971	0.2615	0.5972
	LR-CCSD	0.1340	0.2820	0.3622	0.2386	0.8034
	EOM-CCSD	0.1340	0.2841	0.3641	0.2399	0.8045
OS	LR-pCCD+S (PCCD)	0.0145	0.1161	0.1700	0.0910	0.2351
	LR-pCCD+S (HF)	0.0142	0.2094	0.1706	0.0878	0.2301
	LR-CCSD	0.0268	0.1238	0.0960	0.0755	0.2921
	EOM-CCSD	0.0268	0.1247	0.0965	0.0759	0.2925
		cc-pVTZ				
		1b <sub>1</sub> → 4a <sub>1</sub>	1b <sub>2</sub> → 2b <sub>2</sub>	3a <sub>1</sub> → 4a <sub>1</sub>	3a <sub>1</sub> → 2b <sub>2</sub>	1b <sub>2</sub> → 4a <sub>1</sub>
EE	LR-pCCD+S (pCCD)	0.3988	0.6510	0.4295	0.5090	0.5706
	LR-pCCD+S (HF)	0.3486	0.6364	0.4290	0.5025	0.5540
	LR-CCSD	0.2977	0.6304	0.3895	0.4652	0.5328
	EOM-CCSD	0.2977	0.6304	0.3895	0.4652	0.5328
	CCSDR(3)	0.2979	0.6292	0.3894	0.4652	0.5321
TDM	LR-pCCD+S (pCCD)	0.488	0.599	0.794	0.5391	0.7737
	LR-pCCD+S (HF)	0.478	0.5001	0.7938	0.4902	0.7333
	LR-CCSD	0.4341	0.4428	0.6359	0.4361	0.8204
	EOM-CCSD	0.4335	0.4446	0.638	0.4384	0.8215
DS	LR-pCCD+S (pCCD)	0.2381	0.3588	0.6304	0.2906	0.5986
	LR-pCCD+S (HF)	0.2285	0.2501	0.6301	0.2403	0.5377
	LR-CCSD	0.1884	0.1961	0.4044	0.1902	0.6731
	EOM-CCSD	0.1879	0.1977	0.4071	0.1922	0.6748
OS	LR-pCCD+S (PCCD)	0.0633	0.1557	0.1805	0.0986	0.2277
	LR-pCCD+S (HF)	0.0531	0.1061	0.1802	0.0805	0.1986
	LR-CCSD	0.0374	0.0824	0.1050	0.0590	0.2391
	EOM-CCSD	0.0373	0.0831	0.1057	0.0596	0.2397
		cc-pVQZ				
		1b <sub>1</sub> → 4a <sub>1</sub>	1b <sub>2</sub> → 2b <sub>2</sub>	3a <sub>1</sub> → 4a <sub>1</sub>	3a <sub>1</sub> → 2b <sub>2</sub>	1b <sub>2</sub> → 4a <sub>1</sub>
EE	LR-pCCD+S (pCCD)	0.3624	0.6563	0.4270	0.5162	0.6353
	LR-pCCD+S (HF)	0.3417	0.6383	0.4068	0.4935	0.6158
	LR-CCSD	0.2949	0.6121	0.3847	0.4582	0.5274
	EOM-CCSD	0.2949	0.6121	0.3847	0.4582	0.5274
	CCSDR(3)	0.2944	0.6111	0.3840	0.4579	0.5264
TDM	LR-pCCD+S (pCCD)	0.6529	0.5280	0.6861	0.8363	0.8879
	LR-pCCD+S (HF)	0.5187	0.4472	0.7929	0.7878	0.7714
	LR-CCSD	0.4795	0.3785	0.6510	0.4021	0.7677
	EOM-CCSD	0.4794	0.3796	0.6531	0.4042	0.7685
DS	LR-pCCD+S (pCCD)	0.4263	0.2788	0.4707	0.6994	0.7884
	LR-pCCD+S (HF)	0.2691	0.2000	0.6287	0.6207	0.5951
	LR-CCSD	0.2299	0.1433	0.4238	0.1617	0.5893
	EOM-CCSD	0.2298	0.1441	0.4266	0.1634	0.5906
OS	LR-pCCD+S (pCCD)	0.1030	0.1220	0.1340	0.2407	0.3339
	LR-pCCD+S (HF)	0.0613	0.0851	0.1705	0.2042	0.2443
	LR-CCSD	0.0452	0.0585	0.1087	0.0494	0.2072
	EOM-CCSD	0.0452	0.0588	0.1094	0.0499	0.2077

		aug-cc-pVTZ				
Property	Method	$1b_1 \rightarrow 4a_1$	$1b_2 \rightarrow 2b_2$	$3a_1 \rightarrow 4a_1$	$3a_1 \rightarrow 2b_2$	$1b_2 \rightarrow 4a_1$
EE	LR_pCCDS(pCCD)	0.3480	0.4605	0.4093	0.4789	0.5377
	LR_pCCDS(HF)	0.3261	0.4402	0.3872	0.4602	0.5113
	LR-CCSD	0.2792	0.4175	0.3659	0.4298	0.4878
	EOM-CCSD	0.2792	0.4175	0.3659	0.4298	0.4957
	CCSDR(3)	0.2792	0.4177	0.3659	0.4305	0.4885
TDM	LR_pCCDS(pCCD)	0.7712	0.1411	0.7835	0.4199	0.3111
	LR_pCCDS(HF)	0.7424	0.1196	0.7407	0.3111	0.4970
	LR-CCSD	0.5362	0.0200	0.6346	0.2415	0.4223
	EOM-CCSD	0.5364	0.0600	0.6365	0.2425	0.4268
DS	LR_pCCDS(pCCD)	0.5948	0.0199	0.6139	0.1763	0.0968
	LR_pCCDS(HF)	0.5511	0.0143	0.5486	0.0968	0.2470
	LR-CCSD	0.2875	0.0004	0.4027	0.0583	0.1783
	EOM-CCSD	0.2877	0.0036	0.4051	0.0588	0.1822
OS	LR_pCCDS(pCCD)	0.1380	0.0061	0.1675	0.0563	0.0347
	LR_pCCDS(HF)	0.1198	0.0042	0.1416	0.0297	0.0842
	LR-CCSD	0.0535	0.0001	0.0982	0.0167	0.0580
	EOM-CCSD	0.0535	0.0010	0.0988	0.0168	0.0602

Table S4: Vertical excitation energies (EE), TDMs, DSs, and OSs for furan in ground state geometry using cc-pVDZ, cc-pVTZ, cc-pVQZ and aug-cc-pVTZ basis sets.

		cc-pVDZ					
Property	Method	$1a_2 \rightarrow 7b_2$	$8a_1 \rightarrow 3b_2$	$1b_1 \rightarrow 3b_2$	$6b_2 \rightarrow 10a_1$	$1b_1 \rightarrow 2a_2$	$8a_1 \rightarrow 8b_2$
EE	LR-pCCD+S (pCCD)	0.3310	0.3930	0.4457	0.4992	0.5113	0.5391
	LR-pCCD+S (HF)	0.3228	0.3926	0.4428	0.5095	0.5127	0.5355
	LR-CCSD	0.3311	0.3870	0.4356	0.4957	0.5106	0.5304
	EOM-CCSD	0.3311	0.3870	0.4356	0.4957	0.5106	0.5304
	CCSDR(3)	0.3281	0.3820	0.4176	0.4910	0.4958	0.5230
TDM	LR-pCCD+S (pCCD)	0.3681	0.1934	0.7434	0.9985	1.0096	0.7622
	LR-pCCD+S (HF)	0.2963	0.1054	0.8498	0.9732	0.9244	0.9208
	LR-CCSD	0.6143	0.0200	0.6806	1.1561	1.1317	0.9117
	EOM-CCSD	0.6158	0.0000	0.6752	1.1574	1.1436	0.9123
DS	LR-pCCD+S (pCCD)	0.1355	0.0374	0.5526	0.9970	1.0192	0.5810
	LR-pCCD+S (HF)	0.0878	0.0111	0.7222	0.9471	0.8546	0.8479
	LR-CCSD	0.3774	0.0004	0.4632	1.3366	1.2808	0.8312
	EOM-CCSD	0.3792	0.0000	0.4559	1.3396	1.3079	0.8323
OS	LR-pCCD+S (PCCD)	0.0299	0.0098	0.1642	0.3318	0.3474	0.2088
	LR-pCCD+S (HF)	0.0189	0.0029	0.2132	0.3217	0.2921	0.3027
	LR-CCSD	0.0833	0.0001	0.1345	0.4417	0.4360	0.2939
	EOM-CCSD	0.0837	0.0000	0.1324	0.4427	0.4452	0.2943
		cc-pVTZ					
		$1a_2 \rightarrow 7b_2$	$8a_1 \rightarrow 3b_2$	$1b_1 \rightarrow 3b_2$	$6b_2 \rightarrow 10a_1$	$1b_1 \rightarrow 2a_2$	$8a_1 \rightarrow 8b_2$
EE	LR-pCCD+S (pCCD)	0.3381	0.3653	0.4346	0.4773	0.4987	0.5025
	LR-pCCD+S (HF)	0.3515	0.3715	0.4318	0.4783	0.4836	0.5363
	LR-CCSD	0.3073	0.3647	0.4301	0.4717	0.4872	0.5027
	EOM-CCSD	0.3073	0.3647	0.4302	0.4717	0.4873	0.5030
	CCSDR(3)	0.3044	0.3605	0.4125	0.4671	0.4806	0.4883
TDM	LR-pCCD+S (pCCD)	0.3599	0.3305	0.6836	0.4062	0.3077	0.3554
	LR-pCCD+S (HF)	0.3432	0.2748	0.6785	0.6368	0.22	0.2035
	LR-CCSD	0.783	0.1892	0.6402	0.9522	0.2707	0.2406
	EOM-CCSD	0.7852	0.1913	0.6344	0.9557	0.2694	0.2478
DS	LR-pCCD+S (pCCD)	0.1295	0.1092	0.4673	0.1650	0.0947	0.1263
	LR-pCCD+S (HF)	0.1178	0.0755	0.4603	0.4055	0.0484	0.0414
	LR-CCSD	0.6131	0.0358	0.4098	0.9066	0.0733	0.0579
	EOM-CCSD	0.6165	0.0366	0.4024	0.9133	0.0726	0.0614
OS	LR-pCCD+S (PCCD)	0.0292	0.0266	0.1354	0.0525	0.0315	0.0423
	LR-pCCD+S (HF)	0.0276	0.0187	0.1325	0.1293	0.0156	0.0148
	LR-CCSD	0.1256	0.0087	0.1175	0.2851	0.0238	0.0194
	EOM-CCSD	0.1263	0.0089	0.1154	0.2872	0.0236	0.0206
		cc-pVQZ					
		$1a_2 \rightarrow 7b_2$	$8a_1 \rightarrow 3b_2$	$1b_1 \rightarrow 3b_2$	$6b_2 \rightarrow 10a_1$	$1b_1 \rightarrow 2a_2$	$8a_1 \rightarrow 8b_2$
EE	LR-pCCD+S (pCCD)	0.3189	0.3653	0.4432	0.4822	0.5035	0.5189
	LR-pCCD+S (HF)	0.3228	0.3750	0.4307	0.4740	0.4958	0.5213
	LR-CCSD	0.2910	0.3630	0.4286	0.4461	0.4669	0.4819
	EOM-CCSD	0.2910	0.3630	0.4286	0.4461	0.4669	0.4819
	CCSDR(3)	0.3133	0.3515	0.4215	0.4415	0.4772	0.4910
TDM	LR-pCCD+S (pCCD)	0.4682	0.3033	0.4207	1.2361	0.9446	0.5384
	LR-pCCD+S (HF)	0.4583	0.3453	0.3451	1.1902	0.8126	0.3701
	LR-CCSD	0.1572	0.1364	0.6179	1.3460	1.1515	0.1476
	EOM-CCSD	0.1622	0.1393	0.5981	1.3461	1.1519	0.1487
DS	LR-pCCD+S (pCCD)	0.2192	0.0920	0.1770	1.5280	0.8923	0.2899
	LR-pCCD+S (HF)	0.2100	0.1192	0.1191	1.4165	0.6604	0.1370
	LR-CCSD	0.0247	0.0186	0.3818	1.8117	1.3259	0.0218
	EOM-CCSD	0.0263	0.0194	0.3577	1.8120	1.3268	0.0221
OS	LR-pCCD+S (PCCD)	0.0466	0.0224	0.0523	0.4912	0.2995	0.1003
	LR-pCCD+S (HF)	0.0452	0.0298	0.0342	0.4476	0.2183	0.0476
	LR-CCSD	0.0048	0.0045	0.1091	0.5388	0.4127	0.0070
	EOM-CCSD	0.0051	0.0047	0.1022	0.5389	0.4130	0.0071

		aug-cc-pVTZ					
Property	Method	$1a_2 \rightarrow 7b_2$	$8a_1 \rightarrow 3b_2$	$1b_1 \rightarrow 3b_2$	$6b_2 \rightarrow 10a_1$	$1b_1 \rightarrow 2a_2$	$8a_1 \rightarrow 8b_2$
EE	LR-pCCD+S (pCCD)	0.3189	0.4432	0.3653	0.4822	0.5035	0.5189
	LR-pCCD+S (HF)	0.2434	0.3268	0.3198	0.3307	0.4059	0.4097
	LR-CCSD	0.2465	0.3225	0.3079	0.3306	0.4007	0.4097
	EOM-CCSD	0.2465	0.3225	0.3079	0.3306	0.4007	0.4097
	CCSDR(3)	0.2444	0.3198	0.3016	0.3264	0.3972	0.4077
TDM	LR-pCCD+S (pCCD)	0.3904	0.3971	0.4175	0.5066	0.3947	0.3697
	LR-pCCD+S (HF)	0.4717	0.4988	0.8843	0.7793	0.4610	0.3138
	LR-CCSD	0.4909	0.2390	1.3828	0.8347	0.2733	0.1806
	EOM-CCSD	0.4934	0.2415	1.4179	0.8594	0.2722	0.1758
DS	LR-pCCD+S (pCCD)	0.1524	0.1577	0.1743	0.2566	0.1558	0.1367
	LR-pCCD+S (HF)	0.2225	0.2488	0.7819	0.6073	0.2125	0.0985
	LR-CCSD	0.2410	0.0571	1.9120	0.6968	0.0747	0.0326
	EOM-CCSD	0.2434	0.0583	2.0103	0.7385	0.0741	0.0309
OS	LR-pCCD+S (pCCD)	0.0324	0.0466	0.0515	0.0825	0.0523	0.0473
	LR-pCCD+S (HF)	0.0361	0.0542	0.1667	0.1339	0.0575	0.0269
	LR-CCSD	0.0396	0.0123	0.3925	0.1536	0.0199	0.0089
	EOM-CCSD	0.0400	0.0125	0.4127	0.1628	0.0198	0.0085

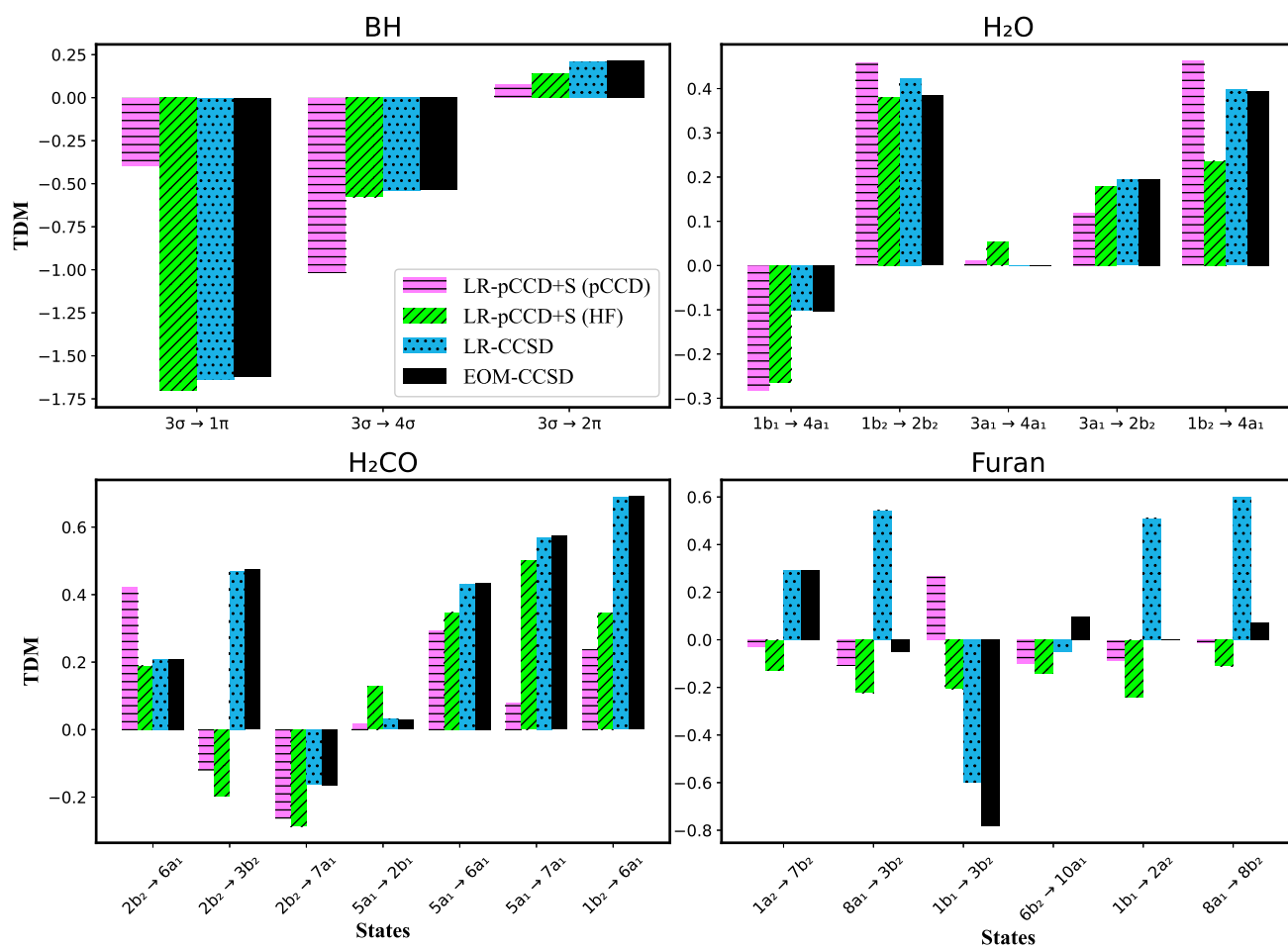


Figure S1: Difference in TDM between the cc-pVTZ and aug-cc-pVTZ basis sets for BH, H<sub>2</sub>O, H<sub>2</sub>CO, and Furan molecules.

Table S5: Mean Absolute Error (MA), Mean Average Error (ME), and Standard Deviation (SD) for the LR-pCCD+S TDM, OS, and DS of BH, H<sub>2</sub>O, H<sub>2</sub>CO, and Furan molecules w.r.t. LR-CCSD. dz, tz, and qz denote cc-pVDZ, cc-pVTZ, and cc-pVQZ basis sets, respectively.

		BH			H <sub>2</sub> O		
Property	Basis	dz	tz	qz	dz	tz	qz
TDM	SD (pCCD) <sup>a</sup>	0.0482	0.0727	0.0285	0.0081	0.0101	0.0198
	SD (HF) <sup>b</sup>	0.0474	0.0250	0.0140	0.0113	0.0062	0.0132
	MAE (pCCD) <sup>c</sup>	0.0878	0.1117	0.0567	0.0179	0.0205	0.0363
	MAE (HF) <sup>d</sup>	0.0931	0.0199	0.0361	0.0234	0.0158	0.0253
DS	SD (pCCD)	0.1282	0.1625	0.0355	0.0106	0.0115	0.0252
	SD (HF)	0.1260	0.0484	0.0303	0.0143	0.0091	0.0169
	MAE (pCCD)	0.2304	0.2294	0.0810	0.0219	0.0243	0.0444
	MAE (HF)	0.2403	0.0494	0.0618	0.0287	0.0200	0.0304
	SD (pCCD)	0.0299	0.0326	0.0069	0.0041	0.0048	0.0103
OS	SD (HF)	0.0301	0.0107	0.0049	0.0181	0.0032	0.0049
	MAE (pCCD)	0.0550	0.0444	0.0158	0.0330	0.0090	0.0185
	MAE (HF)	0.0538	0.0083	0.0115	0.0323	0.0070	0.0118
		H <sub>2</sub> CO			Furan		
TDM	SD (pCCD)	0.0192	0.0139	0.0076	0.0108	0.0227	0.0369
	SD (HF)	0.0131	0.0041	0.0024	0.0143	0.0255	0.0112
	MAE (pCCD)	0.0299	0.0268	0.0118	0.0264	0.0708	0.0536
	MAE (HF)	0.0220	0.0147	0.0061	0.0281	0.0736	0.0340
DS	SD (pCCD)	0.0347	0.0234	0.0137	0.0147	0.0264	0.0588
	SD (HF)	0.0219	0.0076	0.0041	0.0223	0.0284	0.0169
	MAE (pCCD)	0.0477	0.0385	0.0166	0.0339	0.0811	0.0750
	MAE (HF)	0.0351	0.0221	0.0076	0.0387	0.0830	0.0494
OS	SD (pCCD)	0.0127	0.0070	0.0039	0.0049	0.0053	0.0113
	SD (HF)	0.0087	0.0018	0.0017	0.0069	0.0056	0.0034
	MAE (pCCD)	0.0164	0.0124	0.0048	0.0108	0.0162	0.0154
	MAE (HF)	0.0102	0.0066	0.0012	0.0120	0.0164	0.0105

<sup>a</sup>  $SD = \sqrt{\frac{\sum_n (x_n - \bar{x})^2}{N}}$ , and SD(pCCD) is DS for pCCD+S(pCCD) results,  $\bar{x}$  is average over all states and  $N$  is number of states.

<sup>b</sup> SD(HF) is DS for pCCD+S(HF) results.

MAE =  $\frac{1}{N} \sum_n |x_n - x_r|$ , where  $x_r$  is a LR-CCSD results as a reference data.

<sup>c</sup> MAE(pCCD) is MAE, where  $x_a$  = LR-pCCD+S(pCCD) results.

<sup>d</sup> MAE(HF) is MAE, where  $x_a$  = LR-pCCD+S(HF) results.

Table S6: Average of standard deviations (SDs) and mean absolute errors (MAEs) of data in Table S5, over all molecules.

Property	Statistics	cc-pVDZ	cc-pVTZ	cc-pVQZ
TDM	SD (pCCD)	0.0216	0.0299	0.0232
	SD (HF)	0.0215	0.0152	0.0102
	MAE (pCCD)	0.0405	0.0575	0.0396
	MAE (HF)	0.0416	0.0310	0.0254
	SD (pCCD)	0.0470	0.0559	0.0333
DS	SD (HF)	0.0461	0.0234	0.0171
	MAE (pCCD)	0.0835	0.0933	0.0542
	MAE (HF)	0.0857	0.0436	0.0373
	SD (pCCD)	0.0129	0.0124	0.0081
OS	SD (HF)	0.0160	0.0053	0.0037
	MAE (pCCD)	0.0288	0.0205	0.0136
	MAE (HF)	0.0271	0.0096	0.0087



## S2 Deriving the Jacobian matrix elements

To obtain the linear response vectors and matrices, we consider the de-excitation, and excitation operators, summarized in Table 1. The molecular Hamiltonian is defined as

$$\mathbf{H}_0 = \sum_{pq} f_p^q \{\hat{p}^\dagger \hat{q}\} + \frac{1}{2} \sum_{pqrs} V_{pqrs}^{rs} \{\hat{p}^\dagger \hat{q}^\dagger \hat{s} \hat{r}\}, \quad (\text{S1})$$

and the second quantization operator commutation relations are,

$$\begin{aligned} [\hat{p}^\dagger, \hat{P}_b] &= -\hat{b} \delta_{pb}, & [\hat{r}, \hat{P}_i^\dagger] &= \hat{i}^\dagger \delta_{ri}, \\ [\hat{i}^\dagger, \hat{P}_b] &= [\hat{i}, \hat{P}_a^\dagger] = [\hat{a}^\dagger, \hat{P}_i] = [\hat{a}, \hat{P}_i^\dagger] = 0. \end{aligned} \quad (\text{S2})$$

### S2.1 The Jacobian matrix for pair excitations

The Jacobian matrix elements for the pair excitations are as follow

$$\begin{aligned} \mathbf{J}_{\mu_2 \nu_2} &= \mathbf{J}_{iajb}^{(2,2)} = \langle \mu_2 | [\hat{H}_0, \hat{\nu}_2] | \text{HF} \rangle = \langle \text{HF} | \hat{\nu}_2^\dagger [\hat{H}_0, \hat{\nu}_2] | \text{HF} \rangle \\ &+ \sum_{kc} \langle \text{HF} | \hat{\nu}_2^\dagger [[\hat{H}_0, t_{kk}^{c\bar{c}} \hat{\nu}_2], \hat{\nu}_2] | \text{HF} \rangle \\ &= \langle \text{HF} | \hat{P}_i^\dagger \hat{P}_a [\hat{H}_0, \hat{P}_b^\dagger \hat{P}_j] | \text{HF} \rangle \\ &+ \langle \text{HF} | \hat{P}_i^\dagger \hat{P}_a [[\hat{H}_0, \sum_{ck} t_{kk}^{c\bar{c}} \hat{P}_c^\dagger \hat{P}_k], \hat{P}_b^\dagger \hat{P}_j] | \text{HF} \rangle. \end{aligned} \quad (\text{S3})$$

For pair-pair couplings,

$$\begin{aligned} J_{iajb}^{(2,2)} &= \langle \text{HF} | \{\hat{i}^\dagger \hat{i}^\dagger \hat{a} \hat{a}\} \left( \sum_{pq} f_p^q \{\hat{p}^\dagger \hat{q}\} + \frac{1}{4} \sum_{pqrs} V_{pqrs}^{rs} \{\hat{p}^\dagger \hat{q}^\dagger \hat{s} \hat{r}\} \right) \{\hat{b}^\dagger \hat{b}^\dagger \hat{j} \hat{j}\} | \text{HF} \rangle \\ &+ \langle \text{HF} | \{\hat{i}^\dagger \hat{i}^\dagger \hat{a} \hat{a}\} \left( \sum_{pq} f_p^q \{\hat{p}^\dagger \hat{q}\} + \frac{1}{4} \sum_{pqrs} V_{pqrs}^{rs} \{\hat{p}^\dagger \hat{q}^\dagger \hat{s} \hat{r}\} \right) \\ &\sum_{kc} t_{kk}^{c\bar{c}} \{c^\dagger \bar{c}^\dagger \bar{k} k\} \{\hat{b}^\dagger \hat{b}^\dagger \hat{j} \hat{j}\} | \text{HF} \rangle. \end{aligned} \quad (\text{S4})$$

Using Wick's theorem to identify the connected terms, the pCCD Jacobian matrix can be written as

$$\begin{aligned} \mathbf{J}_{iajb}^{(2,2)} &= (2f_a^a - 2f_i^i + 2V_{ia}^{ai} - 4V_{ia}^{ia} - 2 \sum_k V_{kk}^{bb} t_{kk}^{a\bar{a}} \\ &- 2 \sum_c V_j^c t_{ii}^{c\bar{c}} + 4V_{jj}^{bb} t_{ii}^{a\bar{a}}) \delta_{ab} \delta_{ij} \\ &+ (V_{ii}^{jj} - 2V_{jj}^{bb} t_{ii}^{a\bar{a}} + \sum_c V_{jj}^{cc} t_{ii}^{c\bar{c}}) \delta_{ab} \\ &+ (V_{bb}^{aa} - 2V_{jj}^{bb} t_{ii}^{a\bar{a}} + \sum_k V_{kk}^{bb} t_{kk}^{a\bar{a}}) \delta_{ij}. \end{aligned} \quad (\text{S5})$$

## S2.2 The Jacobian matrix for single excitations

Similarly, for single-single couplings,

$$\begin{aligned}
\mathbf{J}_{\mu_1 \nu_1} &= \mathbf{J}_{iajb}^{(1,1)} = \langle \mu_1 | [\hat{H}_0, \hat{\tau}_{\nu_1}] | \text{HF} \rangle = \langle \text{HF} | \hat{\tau}_{\mu_1}^\dagger [\hat{H}_0, \hat{\tau}_{\nu_1}] | \text{HF} \rangle \\
&+ \sum_{kc} \langle \text{HF} | \hat{\tau}_{\mu_1}^\dagger [[\hat{H}_0, t_{kk}^{c\bar{c}} \hat{\tau}_{k_2}], \hat{\tau}_{\nu_1}] | \text{HF} \rangle \\
&= \langle \text{HF} | \hat{i}^\dagger \hat{a} [\hat{H}_0, \hat{b}^\dagger \hat{j}] | \text{HF} \rangle \\
&+ \langle \text{HF} | \hat{i}^\dagger \hat{a} [[\hat{H}_0, \sum_{ck} t_{kk}^{c\bar{c}} \hat{P}_c^\dagger \hat{P}_k], \hat{b}^\dagger \hat{j}] | \text{HF} \rangle, \tag{S6}
\end{aligned}$$

$$\begin{aligned}
\mathbf{J}_{iajb}^{(1,1)} &= (2f_a^b - 2 \sum_k t_{kk}^{c\bar{c}} V_{kk}^{ab}) \delta_{ij} \\
&- 2f_j^i - 2 \sum_c t_{ii}^{c\bar{c}} V_{ij}^{cc} \delta_{ab} \\
&+ 4V_{ja}^{bi} - 2V_{aj}^{bi} + t_{ii}^{a\bar{a}} (4V_{ij}^{ab} - 2V_{ij}^{ba}). \tag{S7}
\end{aligned}$$

## S2.3 The Jacobian matrix for pair-single excitations

For pair-single couplings,

$$\begin{aligned}
\mathbf{J}_{\mu_2 \nu_1} &= \mathbf{J}_{iajb}^{(2,1)} = \langle \mu_2 | [\hat{H}_0, \hat{\tau}_{\nu_1}] | \text{HF} \rangle = \langle \text{HF} | \hat{\tau}_{\mu_2}^\dagger [\hat{H}_0, \hat{\tau}_{\nu_1}] | \text{HF} \rangle \\
&+ \sum_{kc} \langle \text{HF} | \hat{\tau}_{\mu_2}^\dagger [[\hat{H}_0, t_{kk}^{c\bar{c}} \hat{\tau}_{k_2}], \hat{\tau}_{\nu_1}] | \text{HF} \rangle \\
&= \langle \text{HF} | \hat{P}_i^\dagger \hat{P}_a [\hat{H}_0, \hat{P}_b^\dagger \hat{P}_j] | \text{HF} \rangle \\
&+ \langle \text{HF} | \hat{P}_i^\dagger \hat{P}_a [[\hat{H}_0, \sum_{ck} t_{kk}^{c\bar{c}} \hat{P}_c^\dagger \hat{P}_k], \hat{b}^\dagger \hat{j}] | \text{HF} \rangle. \tag{S8}
\end{aligned}$$

$$\begin{aligned}
\mathbf{J}_{iajb}^{(2,1)} &= -2t_{ii}^{a\bar{a}} f_j^a + t_{ii}^{a\bar{a}} (4V_{ij}^{ia} - 2V_{ij}^{ai}) - 4 \sum_c t_{ii}^{c\bar{c}} V_{ja}^{cc} \delta_{ab} \\
&- 2t_{ii}^{a\bar{a}} f_i^b - t_{ii}^{a\bar{a}} (4V_{ai}^{ab} - 2V_{ia}^{ab}) - 4 \sum_k t_{kk}^{a\bar{a}} V_{kk}^{bi} \delta_{ij} \\
&- t_{ii}^{a\bar{a}} (4(V_{aj}^{ab} - V_{ji}^{bi}) - 2(V_{ja}^{ai} - V_{ai}^{ba})). \tag{S9}
\end{aligned}$$

## S2.4 The Jacobian matrix for single-pair excitations

Finally, for single-pair couplings,

$$\begin{aligned}
\mathbf{J}_{\mu_1 \nu_2} &= \mathbf{J}_{iajb}^{(1,2)} = \langle \mu_1 | [\hat{H}_0, \hat{\tau}_{\nu_2}] | \text{HF} \rangle = \langle \text{HF} | \hat{\tau}_{\mu_1}^\dagger [\hat{H}_0, \hat{\tau}_{\nu_2}] | \text{HF} \rangle \\
&+ \sum_{kc} \langle \text{HF} | \hat{\tau}_{\mu_1}^\dagger [[\hat{H}_0, t_{kk}^{c\bar{c}} \hat{\tau}_{k_2}], \hat{\tau}_{\nu_2}] | \text{HF} \rangle \\
&= \langle \text{HF} | \hat{i}^\dagger \hat{a} [\hat{H}_0, \hat{P}_b^\dagger \hat{P}_j] | \text{HF} \rangle \\
&+ \langle \text{HF} | \hat{i}^\dagger \hat{a} [[\hat{H}_0, \sum_{ck} t_{kk}^{c\bar{c}} \hat{P}_c^\dagger \hat{P}_k], \hat{P}_b^\dagger \hat{P}_j] | \text{HF} \rangle. \tag{S10}
\end{aligned}$$

$$\begin{aligned}
J_{iajb}^{(1,2)} &= -2t_{ii}^{a\bar{a}} f_j^a - t_{ii}^{a\bar{a}} (4V_{ij}^{ia} - 2V_{ij}^{ai}) - 4 \sum_c t_{ii}^{c\bar{c}} V_{ja}^{cc} \delta_{ab} \\
&\quad - 2t_{ii}^{a\bar{a}} f_i^b + t_{ii}^{a\bar{a}} (4V_{ai}^{ab} - 2V_{ia}^{ab}) - 4 \sum_k t_{kk}^{a\bar{a}} V_{kk}^{bi} \delta_{ij} \\
&\quad - t_{ii}^{a\bar{a}} (4(V_{aj}^{ab} - V_{ji}^{bi}) - 2(V_{ja}^{ai} - V_{ai}^{ba})).
\end{aligned} \tag{S11}$$

The elements  $J_{\mu_2\nu_2}$ ,  $J_{\mu_1\nu_1}$ ,  $J_{\mu_2\nu_1}$ , and  $J_{\mu_1\nu_2}$  correspond to different excitation types. Each matrix element is derived from the expectation values of the Hamiltonian operator, appropriately expanded with Wick's theorem and commutators. For detailed derivations, refer to the primary coupled-cluster theory literature.

This formalism outlines the construction of the pCCD Jacobian matrix, providing a foundation for further computational implementation and analysis of electron correlation effects in molecular systems. The final Jacobian matrix can be written as,

$$J_{iajb} = \begin{pmatrix} J_{iajb}^{(1,1)} & J_{iajb}^{(1,2)} \\ J_{iajb}^{(2,1)} & J_{iajb}^{(2,2)} \end{pmatrix}. \tag{S12}$$

### S3 Derivation of the $F_{\mu\nu}$ matrix elements

The transition matrix elements for  $F_{\mu\nu}$  (see also Table 1) can be derived using the following equations,

$$F_{\nu k} = \langle \Lambda | [[\hat{H}_0, \hat{\tau}_\nu], \hat{\tau}_k] | \text{pCCD} \rangle, \tag{S13}$$

for pair-pair couplings,

$$\begin{aligned}
F_{\mu_2\nu_2} &= F_{iajb}^{(2,2)} = \langle \Lambda | [[\hat{H}_0, \hat{\tau}_{\mu_2}], \hat{\tau}_{\nu_2}] | \text{pCCD} \rangle \\
&= (t_{ii}^{b\bar{b}} V_{jj}^{aa} + t_{jj}^{a\bar{a}} V_{ii}^{bb}) + 4(t_{aa}^{i\bar{i}} V_{ii}^{aa}) \delta_{ij} \delta_{ab} \\
&\quad - 2(\bar{t}_{bb}^{i\bar{i}} V_{jj}^{aa} + \bar{t}_{aa}^{i\bar{i}} V_{jj}^{bb}) \delta_{ij} \\
&\quad - 2(\bar{t}_{aa}^{i\bar{i}} V_{jj}^{bb} + \bar{t}_{aa}^{j\bar{j}} V_{ii}^{bb}) \delta_{ab}.
\end{aligned} \tag{S14}$$

For single-single couplings,

$$\begin{aligned}
F_{\mu_1\nu_1} &= F_{iajb}^{(1,1)} = \langle \Lambda | [[\hat{H}_0, \hat{\tau}_{\mu_1}], \hat{\tau}_{\nu_1}] | \text{pCCD} \rangle \\
&= -2\bar{t}_{bb}^{i\bar{i}} (2V_{jb}^{ai} - V_{jb}^{ia}) - 2\bar{t}_{aa}^{j\bar{j}} (2V_{ia}^{bj} - V_{ia}^{jb}) \\
&\quad + 2(2V_{ij}^{ab} - V_{ji}^{ab}) + (\bar{t}_{bb}^{i\bar{i}} t_{ii}^{b\bar{b}} + \bar{t}_{aa}^{j\bar{j}} t_{jj}^{a\bar{a}}) (2V_{ji}^{ba} - V_{ji}^{ab}) \\
&\quad - 2 \sum_l \bar{t}_{bb}^{l\bar{l}} t_{li}^{b\bar{b}} (2V_{ij}^{ab} - V_{ji}^{ba}) \\
&\quad + (\sum_{lc} \bar{t}_{cc}^{l\bar{l}} t_{ij}^{c\bar{c}} V_{ij}^{cc} + 2 \sum_d \bar{t}_{dd}^{i\bar{i}} V_{dd}^{ba}) \delta_{ij} \\
&\quad + (\sum_{dk} \bar{t}_{dd}^{j\bar{j}} t_{kk}^{d\bar{d}} V_{kk}^{ba} + 2 \sum_l \bar{t}_{aa}^{l\bar{l}} V_{ji}^{ll}) \delta_{ab}.
\end{aligned} \tag{S15}$$

For single-pair couplings,

$$\begin{aligned}
F_{\mu_1\nu_2} &= F_{iajb}^{(1,2)} = \langle \Lambda | [[\hat{H}_0, \hat{\tau}_{\mu_1}], \hat{\tau}_{\nu_2}] | \text{pCCD} \rangle \\
&= \bar{t}_{aa}^{i\bar{i}} (2V_{ji}^{ai} - 2V_{ij}^{ai} - 2V_{jb}^{aa} + 4V_{ja}^{ba} - 4V_{ji}^{bi}) + 4\bar{t}_{aa}^{j\bar{j}} V_{ii}^{bj} \\
&\quad - 2(\bar{t}_{aa}^{i\bar{i}} (f_i^b + 2V_{ia}^{ba})) \delta_{ij} \\
&\quad - 2\bar{t}_{bb}^{i\bar{i}} f_j^b + 2\bar{t}_{aa}^{i\bar{i}} (2V_{ij}^{ia} - V_{ij}^{ai}) \delta_{ab}.
\end{aligned} \tag{S16}$$

For pair-single couplings,

$$\begin{aligned}
F_{\mu_2\nu_1} &= F_{iajb}^{(2,1)} = \langle \Lambda[[\hat{H}_0, \hat{\tau}_{\mu_2}], \hat{\tau}_{\nu_1}] | \text{pCCD} \rangle \\
&= \bar{t}_{bb}^{jj} (2V_{ij}^{bj} + 2V_{ij}^{ja} + 2V_{jj}^{ia} - 2V_{jb}^{ab} + 2V_{ib}^{ab} - 4V_{ij}^{aj}) \\
&\quad - 2(\bar{t}_{bb}^{jj} (f_j^a + 2V_{jb}^{ab})) \delta_{ij} \\
&\quad - 2(\bar{t}_{aa}^{jj} (f_i^b + 2(V_{ij}^{jb} - V_{ij}^{bj}))) \delta_{ab}.
\end{aligned} \tag{S17}$$

Thus, the  $F_{iajb}$  matrix can be expressed as,

$$F_{iajb} = \begin{pmatrix} F_{iajb}^{(1,1)} & F_{iajb}^{(1,2)} \\ F_{iajb}^{(2,1)} & F_{iajb}^{(2,2)} \end{pmatrix}. \tag{S18}$$

## S4 Derivation of the $\xi_{\hat{V}}^{\hat{A}}$ vector elements

The vector  $\xi_{\hat{V}}^{\hat{A}}$  (Table 1) when  $\hat{A}$  is the dipole operator can be written for pair and single parts, respectively, as the following equations,

$$\begin{aligned}
\xi_{\nu_2}^{\hat{D}} &= \langle \nu_2 | \bar{D} | \text{HF} \rangle = \langle \nu_2 | \hat{D} | \text{HF} \rangle + \langle \nu_2 | \hat{D} \hat{T}_{\text{pCCD}} | \text{HF} \rangle \\
&= 2t_{ii}^{aa} (d_{aa} - d_{ii}),
\end{aligned} \tag{S19}$$

$$\begin{aligned}
\xi_{\nu_1}^{\hat{D}} &= \langle \nu_1 | \bar{D} | \text{HF} \rangle = \langle \nu_1 | \hat{D} | \text{HF} \rangle + \langle \nu_1 | \hat{D} \hat{T}_{\text{pCCD}} | \text{HF} \rangle \\
&= 2t_{ii}^{aa} d_{ia}.
\end{aligned} \tag{S20}$$

Thus, the vector  $\xi_{\hat{V}}^{\hat{D}}$  can be expressed as,

$$\xi_{\hat{V}}^{\hat{D}} = \begin{pmatrix} \xi_{\nu_1}^{\hat{D}} \\ \xi_{\nu_2}^{\hat{D}} \end{pmatrix}. \tag{S21}$$

## S5 Derivation of the $\eta_{\hat{V}}^{\hat{A}}$ vector elements

The vector  $\eta_{\hat{V}}^{\hat{A}}$  (cf. Table 1) when  $\hat{A}$  is the dipole operator and using  $\langle \lambda |$  from Table 1 can be written for pair and single parts, respectively, as

$$\begin{aligned}
\eta_{\nu_2}^{\hat{D}} &= \langle \lambda | [\hat{D}, \hat{\tau}_{\nu_2}] | \text{pCCD} \rangle \\
&= \langle \text{HF} | [\hat{D}, \hat{\tau}_{\nu_2}] | \text{HF} \rangle + \langle \text{HF} | [\hat{D}, \hat{\tau}_{\nu_2}] \hat{T}_{\text{pCCD}} | \text{HF} \rangle \\
&\quad + \sum_{\mu} \bar{t}_{\mu} \langle \mu_2 | [\hat{D}, \hat{\tau}_{\nu_2}] | \text{HF} \rangle + \sum_{\mu} \bar{t}_{\mu} \langle \mu_2 | [[\hat{D}, \hat{\tau}_{\nu_2}], \hat{T}_{\text{pCCD}}] | \text{HF} \rangle \\
&= 2\bar{t}_{bb}^{jj} (d_{bb} - d_{jj}),
\end{aligned} \tag{S22}$$

and

$$\begin{aligned}
\eta_{v_1}^{\hat{D}} &= \langle \lambda | [\hat{D}, \hat{t}_{v_1}] | \text{pCCD} \rangle \\
&= \langle \text{HF} | [\hat{D}, \hat{t}_{v_1}] | \text{HF} \rangle + \langle \text{HF} | [\hat{D}, \hat{t}_{v_1}] \hat{T}_{\text{pCCD}} | \text{HF} \rangle \\
&+ \sum_{\mu} \bar{t}_{\mu} \langle \mu_2 | [\hat{D}, \hat{t}_{v_1}] | \text{HF} \rangle + \sum_{\mu} \bar{t}_{\mu} \langle \mu_2 | [[\hat{D}, \hat{t}_{v_1}], \hat{T}_{\text{pCCD}}] | \text{HF} \rangle \\
&= -2d_{ai} - 2d_{ia} \left( \sum_d t_{ii}^{dd} t_{dd}^{ii} + \sum_l t_{li}^{aa} t_{aa}^{li} \right). \tag{S23}
\end{aligned}$$

Thus, the vector  $\eta_V^{\hat{D}}$  can be expressed as

$$\eta_V^{\hat{D}} = \left( \eta_{v_1}^{\hat{D}}, \quad \eta_{v_2}^{\hat{D}} \right). \tag{S24}$$

## S6 Transition matrix equation

In this section we consider excitation energies and transition moments, which can be obtained based on response functions in coupled cluster theory. We first focus on the exact linear response functions. We assume  $\hat{A}$  and  $\hat{B}$  are Hermitian operators,  $|n\rangle$  and  $E_n$  are defined as exact solutions to the eigenvalue problem of the (time-independent) electronic Hamiltonian  $\hat{H}$  as follows,

$$\hat{H}|n\rangle = E_n|n\rangle. \tag{S25}$$

We number the eigenfunctions and eigenvalues with  $n$  ( $n = 0, 1, 2, \dots$ ), where  $n = 0$  corresponds to the ground state. We also introduce,

$$\omega_n = E_n - E_0, \tag{S26}$$

as the excitation energy from the ground state to the excited state  $n$ . The transition moment, which defines the probability of transition from state  $k$  to state  $n$  due to perturbation  $\hat{B}$ , is given for exact wave functions by the expression

$$T_{kn}^{\hat{B}} = \langle k | \hat{B} | n \rangle. \tag{S27}$$

It follows from this that for exact wave functions,

$$T_{kn}^{\hat{B}} = (T_{nk}^{\hat{B}})^*. \tag{S28}$$

The linear response function can be represented as a sum over states,

$$\langle\langle \hat{A}; \hat{B} \rangle\rangle_{\omega_{\gamma}} = P_{\hat{A}\hat{B}} \sum_{n>0} \frac{\langle 0 | \hat{A} | n \rangle \langle n | \hat{B} | 0 \rangle}{\omega_{\hat{B}} - \omega_n}, \tag{S29}$$

where,  $\gamma = \hat{A}, \hat{B}$  and  $P_{\hat{A}\hat{B}}$  is the sum of permutations of the pairs  $(\hat{A}, \omega_{\hat{A}}), (\hat{B}, \omega_{\hat{B}})$ , remembering that  $\omega_{\hat{A}} + \omega_{\hat{B}} = 0$ . The above formula can be written as,

$$\begin{aligned}
\langle\langle \hat{A}; \hat{B} \rangle\rangle_{\omega} &= \sum_{n>0} \frac{\langle 0 | \hat{A} | n \rangle \langle n | \hat{B} | 0 \rangle}{\omega_{\hat{B}} - \omega_n} + \sum_{n>0} \frac{\langle 0 | \hat{B} | n \rangle \langle n | \hat{A} | 0 \rangle}{\omega_{\hat{A}} - \omega_n}, \\
&= \sum_{n>0} \frac{\langle 0 | \hat{A} | n \rangle \langle n | \hat{B} | 0 \rangle}{\omega_{\hat{B}} - \omega_n} - \sum_{n>0} \frac{\langle 0 | \hat{B} | n \rangle \langle n | \hat{A} | 0 \rangle}{\omega_{\hat{B}} + \omega_n}. \tag{S30}
\end{aligned}$$

From now on, we assume that the frequencies  $\omega$  are real. The linear response function  $\langle\langle \hat{A}; \hat{B} \rangle\rangle_{\omega}$  is a function of frequency  $\omega$ . As a function of frequency, it has first-order poles for values of  $\omega$  equal to the excitation energy  $+\omega_n$  and de-excitation energy  $-\omega_n$

(at these points, some denominators in the sum-over-states expansion above become zero). From the residuals of the function  $\langle\langle\hat{A};\hat{B}\rangle\rangle_\omega$ , we can obtain transition moments as follows,

$$\begin{aligned} & \lim_{\omega \rightarrow \omega_k} (\omega - \omega_k) \langle\langle\hat{A};\hat{B}\rangle\rangle_\omega = \\ & \sum_{n>0} \lim_{\omega \rightarrow \omega_k} \frac{\omega - \omega_k}{\omega - \omega_n} \langle 0|\hat{A}|n\rangle \langle n|\hat{B}|0\rangle - \\ & \sum_{n>0} \lim_{\omega \rightarrow \omega_k} \frac{\omega - \omega_k}{\omega + \omega_n} \langle 0|\hat{B}|n\rangle \langle n|\hat{A}|0\rangle = \langle 0|\hat{A}|k\rangle \langle k|\hat{B}|0\rangle \end{aligned} \quad (\text{S31})$$

This passage to the limit as  $\omega \rightarrow \omega_k$  omits all terms of the expansion except for the first in the first sum, where  $n = k$ . Hence,

$$\frac{\omega - \omega_k}{\omega - \omega_n} = 1. \quad (\text{S32})$$

The obtained term is element of the transition matrix,

$$\Gamma_{0k}^{\hat{A}\hat{B}} = \lim_{\omega \rightarrow \omega_k} (\omega - \omega_k) \langle\langle\hat{A};\hat{B}\rangle\rangle_\omega = \underbrace{\langle 0|\hat{A}|k\rangle}_{T_{0k}^{\hat{A}}} \underbrace{\langle k|\hat{B}|0\rangle}_{T_{k0}^{\hat{B}}}, \quad (\text{S33})$$

where  $T_{0k}$  ( $T_{k0}$ ) is known as the right (left) transition matrix.